

1

Upscaling aquifer storage 2 and recovery (ASR)

3 A northern Ghana multiple case study
4 on small scale agriculture

5 by

6 Frank J. van den Toorn

7 to obtain the degree of Master of Science
8 at the Delft University of Technology,
9 to be defended publicly on Tuesday January 1, 2013 at 10:00 AM.

10 Student number: 4179404
Project duration: September 18, 2017 – July 1, 2018
Thesis committee: Prof. dr. ir. M. Bakker, TU Delft (Chair)
Prof. dr. ir. N.C. van de Giesen, TU Delft
Dr. ir. J.S. Timmermans, TU Delft
Ir. D.A. Brakenhoff, Witteveen+Bos

11 An electronic version of this thesis is available at <http://repository.tudelft.nl/>.



Preface

14 This thesis accommodates the final product in becoming a Master of Science in Watermanagement at the
 15 Delft University of Technology - faculty of Civil Engineering and Geosciences. I would like to acknowledge
 16 all the people who contributed to my graduation. Some however do deserve a special emphasis. First of
 17 all, I would like to thank the entire committee for assessing my thesis. Subsequently I would like to give
 18 a word of gratitude to Witteveen+Bos - Herman Mondeel & Davíd Brakenhoff - for the abundant research
 19 facilities and daily supervision. And last but not least I owe Conservation Alliance - Paa Kofi Osei-Owusu -
 20 a special gratitude. Without the cooperation of CA the fieldwork data collection within the northern Ghana
 21 local communities would not have been possible.

22
23

*Frank J. van den Toorn
Delft, July 2018*



Summary

25 bllaa bbllaa

26

27 enzovort

Contents

29	List of Figures	ix
30	List of Tables	xi
31	1 Introduction	1
32	1.1 Northern Ghana characteristics	1
33	1.2 ASR systems	1
34	1.3 PIT & Irrigation purpose	1
35	2 Fieldwork data analysis	5
36	2.1 Parameter derivation methods	6
37	2.1.1 Theoretical model definition	6
38	2.1.2 Techniques in analysis	6
39	2.1.3 Optimization functions	7
40	2.2 From fieldwork data to T & S values.	9
41	2.2.1 Location: Bingo	9
42	2.2.2 Location: Nungo	9
43	2.2.3 Location: Nyong Nayili	10
44	2.2.4 Location: Janga (1/2)	10
45	2.2.5 Location: Janga (2/2)	11
46	2.2.6 Location: Ziong (monitoring)	11
47	2.3 Theoretical validation	11
48	2.4 Fieldwork results	12
49	3 Model scenarios	13
50	3.1 Scenarios	13
51	3.2 Test criteria	13
52	3.3 Run	13
53	3.4 Results & Conclusions	13
54	4 (Financial) yields - upscaling	15
55	4.1 inhoud	15
56	5 Conclusions	17
57	6 Discussion & Recommendations	19
58	Bibliography	21
59	Appendices	23
60	A Original Borehole Logsheets	25
61	B Fieldwork set-up	31
62	B.1 Equipment	31
63	B.2 General measurement structure	33
64	B.3 Site-specific measurement results	36
65	C Extense report - Fieldwork data analysis	43
66	C.1 Bingo - overview	44
67	C.2 Nungo - overview	46
68	C.3 Nyong Nayili - overview	47
69	C.4 Janga first attempt - overview	49

70	C.5 Janga second attempt - overview	51
71	C.6 Ziong - overview	53
72	D Modflow radial conversion	55
73	D.1 Test 1: Steady flow to a fully penetrating well in confined aquifer	58
74	D.2 Test 2: Steady flow to a fully penetrating well in unconfined aquifer	60
75	D.3 Test 3: Unsteady flow to a partially penetrating well in unconfined aquifer	62

List of Figures

77	1.1 Example on (a) flood near Weisi, Upper West Region and (b) drought near Nungo, Upper East Region	2
78	1.2 Principle Aquifer Storage & Recovery (ASR) system	3
79	1.3 Schematic: dry season system use	3
80	1.4 Schematic: desired up-scaling in dry season system use	3
82	2.1 Overview northern Ghana fieldwork locations	5
83	2.2 Schematic cross-sectional view of (a) generalized northern Ghana soil stratification versus simplified (b) single layered, (c) double layered and (d) partially penetrating double layered approaches in fieldwork data analysis	6
85	2.3 Bingo - multi-layer best fits	9
87	2.4 Nyong Nayili - multi-layer best fits	10
88	2.5 Janga first attempt - multi-layer best fits	10
89	2.6 Janga second attempt - multi-layer best fits	11
90	2.7 Ziong - multi-layer best fits	11
91	B.1 Comparable example of the fieldwork submersible pump	31
92	B.2 Comparable example of the fieldwork generator	32
93	B.3 Actual fieldwork hose & bucket	32
94	B.4 Comparable examples of Van Essen TD- & Baro-Divers	33
95	B.5 Comparable examples of In-Situ TD- & Baro-Divers	33
96	B.6 Comparable example of the fieldwork water tape	34
97	B.7 Fieldwork (measurement) set-up (a) general, (b) simplified	35
98	B.8 Fieldwork fact-sheet: Bingo	37
99	B.9 Fieldwork fact-sheet: Nungo	38
100	B.10 Fieldwork fact-sheet: Nyong Nayili	39
101	B.11 Fieldwork fact-sheet: Janga (attempt 1)	40
102	B.12 Fieldwork fact-sheet: Jamga (attempt 2)	41
103	B.13 Fieldwork fact-sheet: Ziong (location of monitoring)	42
104	C.1 Bingo single layer fieldwork data analysis by the optimization (a) fmin-RMSE method and (b) TTIm calibration method	44
105	C.2 Bingo double layer fieldwork data analysis by the optimization (a) fmin-RMSE method and (b) TTIm calibration method	44
106	C.3 Bingo partially penetrating double layer fieldwork data analysis by the optimization (a) fmin-RMSE method and (b) TTIm calibration method	45
107	C.4 Nyong Nayili single layer fieldwork data analysis by the optimization (a) fmin-RMSE method and (b) TTIm calibration method	47
108	C.5 Nyong Nayili double layer fieldwork data analysis by the optimization (a) fmin-RMSE method and (b) TTIm calibration method	47
109	C.6 Nyong Nayili partially penetrating double layer fieldwork data analysis by the optimization (a) fmin-RMSE method and (b) TTIm calibration method	48
110	C.7 Janga first attempt single layer fieldwork data analysis by the optimization (a) fmin-RMSE method and (b) TTIm calibration method	49
111	C.8 Janga first attempt double layer fieldwork data analysis by the optimization (a) fmin-RMSE method and (b) TTIm calibration method	49

120 C.9 Janga first attempt partially penetrating double layer fieldwork data analysis by the optimiza-	50
121 tion (a) fmin-RMSE method and (b) TTim calibration method	
122 C.10 Janga second attempt single layer fieldwork data analysis by the optimization (a) fmin-RMSE	51
123 method and (b) TTim calibration method	
124 C.11 Janga second attempt double layer fieldwork data analysis by the optimization (a) fmin-RMSE	51
125 method and (b) TTim calibration method	
126 C.12 Janga second attempt partially penetrating double layer fieldwork data analysis by the opti-	52
127 mization (a) fmin-RMSE method and (b) TTim calibration method	
128 C.13 Ziong single layer fieldwork data analysis by the optimization (a) fmin-RMSE method and (b)	53
129 TTim calibration method	
130 C.14 Ziong double layer fieldwork data analysis by the optimization (a) fmin-RMSE method and (b)	53
131 TTim calibration method	
132 C.15 Ziong partially penetrating double layer fieldwork data analysis by the optimization (a) fmin-	54
133 RMSE method and (b) TTim calibration method	
134 D.1 Schematic of an axially symmetric model (Langevin, 2008)	55
135 D.2 Modflow topview schematisation of a: (a) Rectangular model, (b) Rectangular round model	
136 and (c) Single row model	57
137 D.3 Schematic test 1	58
138 D.4 Results test 1	59
139 D.5 Schematic test 2	60
140 D.6 Results test 2	61
141 D.7 Schematic test 3	62
142 D.8 Results test 3: Cross-section head contour after 1 day of pumping	62
143 D.9 Results test 3: Head after 1 day of pumping at 2.0m (relative to aquifer bottom)	63

List of Tables

144

145	2.1 Bingo - overview best fit parameters	9
146	2.2 Nyong Nayili - overview best fit parameters	10
147	2.3 Janga first attempt - overview best fit parameters	10
148	2.4 Janga second attempt - overview best fit parameters	11
149	2.5 Ziong - overview best fit parameters	11

150

151

Introduction

152 **1.1. Northern Ghana characteristics**

153 Ghana's northern part climate is labelled as semi-arid savannah-like. High temperatures are common and
154 on a yearly basis the short rainy season is out-performed by long periods of drought. As a source of water
155 supply, groundwater is abstracted from its surroundings. The relatively high-quality water is collected and
156 mainly used for domestic purposes, livestock and construction. In more restricted quantities groundwater
157 is used for irrigation. The use of groundwater prevents farmers from incurring potential losses in crop pro-
158 duction and increases yields.

159 For as long as natural recharge rates exceed discharge, the used groundwater is renewable and the water
160 source is stated to be sustainable. It is roughly estimated the environment has the capability to naturally
161 recharge a maximum of 2.5-10% of the annual rainfall. Based on the rainfall data for northern Ghana this
162 results in an estimated long term annual natural recharge of 60 mm/y. Currently, local groundwater use is
163 estimated to be approximately 5% of this annual recharge (Martin, 2006). The amount of water withdrawn is
164 marginal and the environment is therefore self-reliant. However, fluctuations in groundwater use over time
165 and place do occur. Accurate field data on these fluctuations is lacking. Recent observations show wells
166 drying out and groundwater tables falling, both indicators of possible unsustainable groundwater use.

167 Following the trend seen in previous decades, it is expected future groundwater production will further
168 increase. An overall improvement of the Ghanaian energy network as well as lower energy costs will make
169 groundwater more accessible via electrical pumps. In general, this will lead to more extensive use of ground-
170 water in the ongoing battle against shortages in clean drinking water. On top of this the national government
171 aims at becoming more self-sufficient. Policies are pointed at more intensive agricultural development in
172 the northern regions of Ghana (Wood, 2013). Optimization in field irrigation has the potential to increase
173 yields and even double the number of crops produced per year (Owusu et al., 2017). Consequently, the need
174 for groundwater abstraction becomes substantially higher. Climate change can potentially have a negative
175 influence on the natural recharge. While the need will be higher, natural recharge volumes can become
176 lower. In the near future it is possible that discharge rates will exceed natural recharge and the abstracting
177 of groundwater is no longer sustainable. Objective of this research is to explore the possibilities of scaling
178 up artificially managed aquifer recharge (MAR) for aquifer storage and recovery (ASR) to contribute towards
179 the continued sustainable use of groundwater in the northern regions of Ghana.

180 **1.2. ASR systems**

181 blabla

182

183 **1.3. PIT & Irrigation purpose**

184 PIT application on irrigation (single figure). and the desired upscaling of this system (multiple figure).
185 resulting in a research question



(a)



(b)

Figure 1.1: Example on (a) flood near Weisi, Upper West Region (source: Owusu et al., 2017) and (b) drought near Nungo, Upper East Region

186 **Background**

187 **Research gap**

188 **Research purpose**

189 **Research question**

190 How can scaled-up Aquifer Storage and Recovery (ASR) systems be beneficial for the availability and sus-
191 tainable use of agricultural groundwater in northern Ghana?

192

193 How can scaled-up Aquifer Storage and Recovery (ASR) systems be beneficial for the availability and sus-
194 tainable use of groundwater in northern Ghana agriculture?

195 **Reader's guide** to answer this research question...

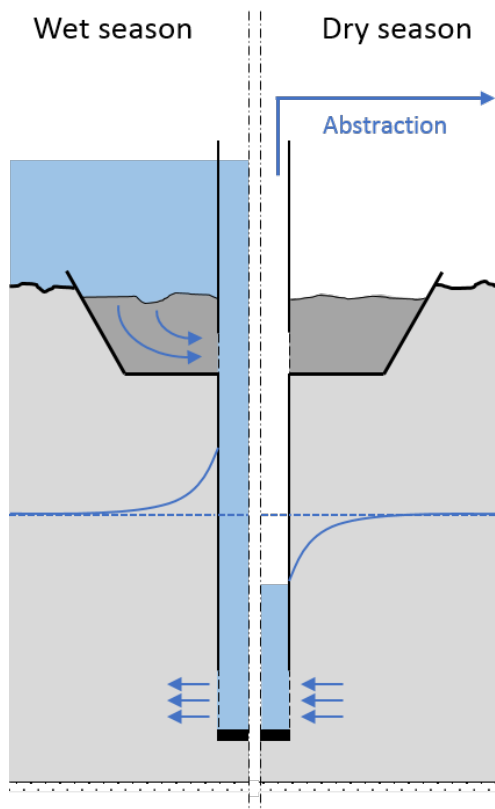


Figure 1.2: Principle Aquifer Storage & Recovery (ASR) system

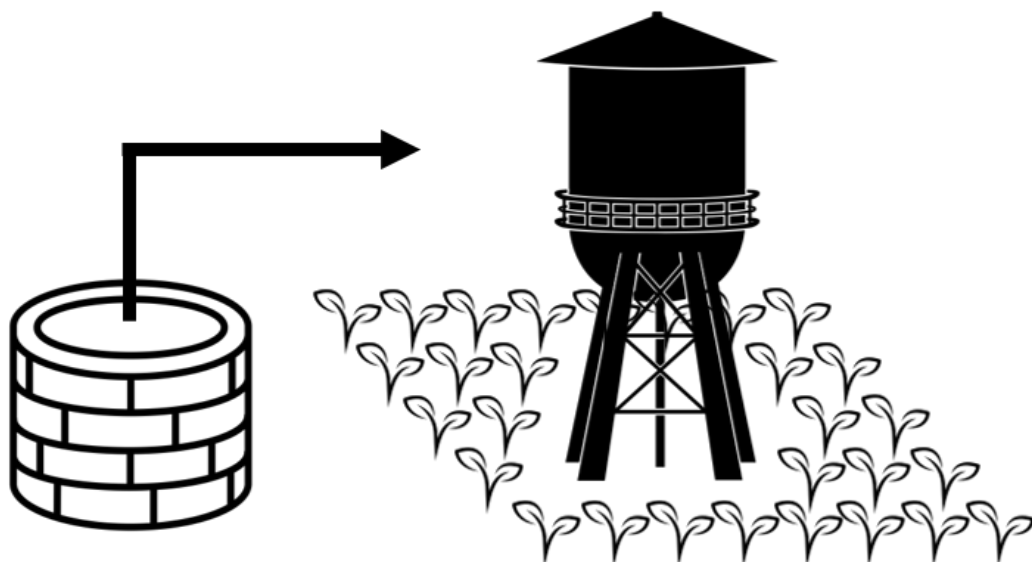


Figure 1.3: Schematic: dry season system use
(visual support by Housin Aziz, Jhun Capaya and Nibras@design from Noun Project - <https://thenounproject.com>)



Figure 1.4: Schematic: desired up-scaling in dry season system use
(visual support by Housin Aziz, Jhun Capaya and Nibras@design from Noun Project - <https://thenounproject.com>)

2

196

197

Fieldwork data analysis

198 Geological conditions are highly heterogeneous in the northern regions of Ghana. Subsurface character-
199 istics vary at short mutual distances. Inadequate and reliable local geohydrological information is preferably
200 gathered by data collection through site-specific fieldwork. In this research perspective, multiple northern
201 Ghana borehole locations are subjected to groundwater pumping tests.

202 Spread over the Upper East and Northern Region the NGO Conservation Alliance (CA) holds several PIT
203 locations, all originated in the summer of 2016. Four of these boreholes are by exception opened for the ap-
204 plication of five pumping tests. A fifth PIT borehole (Ziong) has been made available for the monitoring of
205 the ASR system-use by farmers. The figure below accommodates a map overview of the research locations
206 within northern Ghana (Figure 2.1).

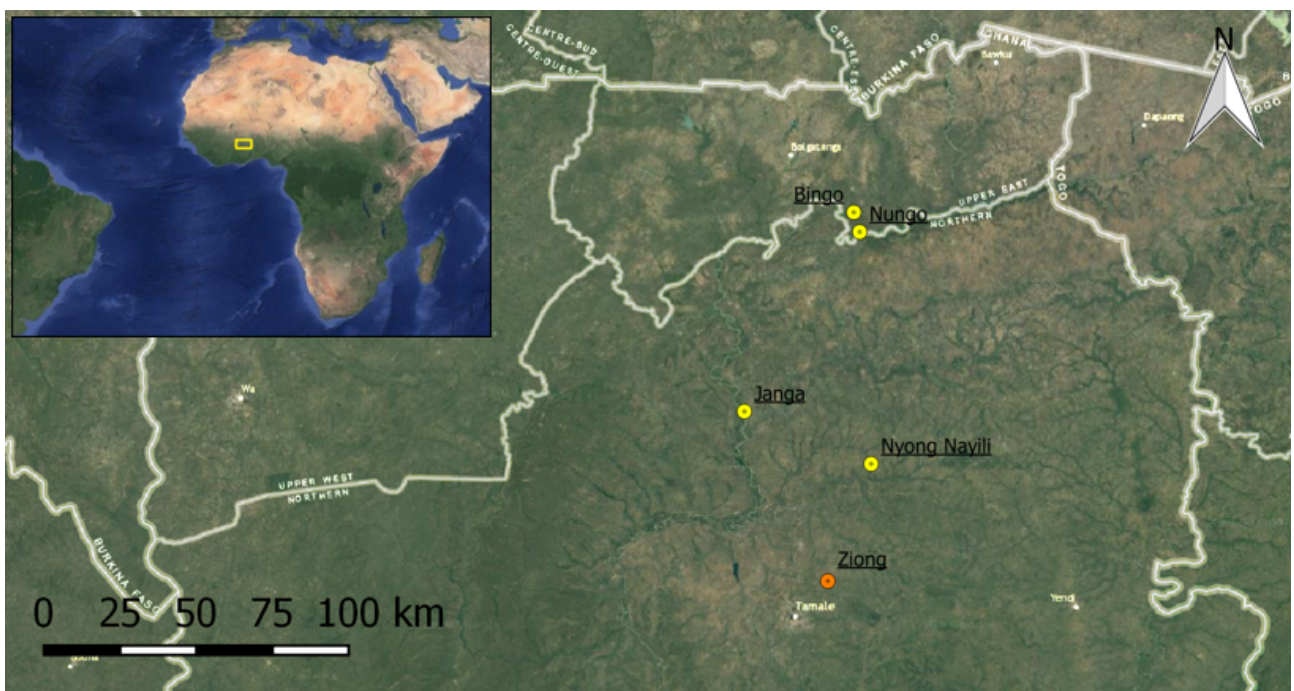


Figure 2.1: Overview northern Ghana fieldwork locations

207 Detailed information on the used equipment and set-up of both the fieldwork pumping tests as well as the
208 groundwate monitoring network (during daily ASR system-use) can be found in appendix B. The obtained
209 raw fieldwork data can be found in the site-specific fact-sheets of appendix B.3. Gathered data acts as input
210 in the derivation of the northern Ghana local geohydrological subsurface parameters; transmissivity (T)
211 (hydraulic conductivity (k)) and storativity (S). 

This chapter accommodates the analysis and processing of gathered fieldwork data. First of all the (simplified) approach in data analysis, including the coherent theoretical background, is explained (section 2.1). Section 2.2 contains the actual derivation of the site-specific groundwater parameter values: T and S. The chapter concludes with the determination of parameter bandwidths (section 2.4), applicable for the further purposes of this research; the model simulation and upscaling of northern Ghana ASR system-use.



2.1. Parameter derivation methods

2.1.1. Theoretical model definition

Large parts of the northern Ghana geohydrological soil characteristics are undetermined. Strong variations in the geological conditions ensures the necessity of local knowledge in soil stratification. Most reliable site-specific information is recorded during borehole construction (2016). Content of the borehole log-sheets, available for the five research locations in appendix A, is used as a starting point in the theoretical model determination.



Despite differences in present soil types, the research locations show similarities in stratification. In each case the soil top structure (approximately 50 m) is roughly divided into two or three layers (confining top layer). Groundwater tables are predominantly positioned in the first aquifer (layer under confining layer). Result is the selection of multiple (three in total) simplified theoretical models for the fieldwork data analysis, as depicted in figure 2.2.

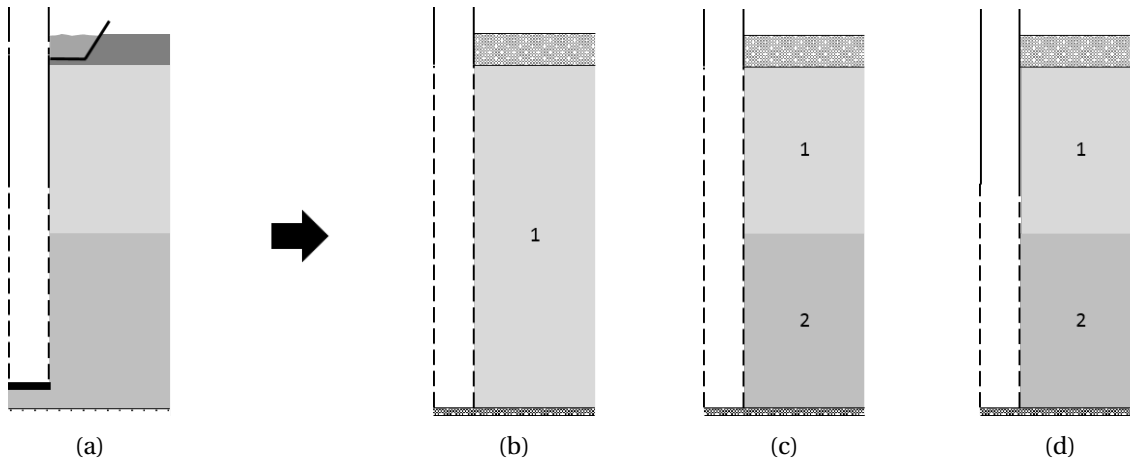


Figure 2.2: Schematic cross-sectional view of (a) generalized northern Ghana soil stratification versus simplified (b) single layered, (c) double layered and (d) partially penetrating double layered approaches in fieldwork data analysis

These simplified models (2.2b - 2.2d) mimic local circumstances, making the derivation of representative hydraulic subsurface characteristics (T and S) possible (Kruseman & de Ridder, 2000). Extension in the number of layers provides more degrees of freedom. Causing a double layered models to potentially simulate the gathered fieldwork data with higher accuracies. To limit chances of equifinality a maximum of two soil layers are implemented.

235

2.1.2. Techniques in analysis

Increased number of layers, and the degrees of freedom, suggest a gain in parameter derivation complexity. To enable the derivation of (multiple) hydraulic groundwater parameters, different suitable methods are applied. This section contains a detailed description of techniques applied.



240

Analytical: Theis's method

Groundwater drawdown due to the withdrawal of water can analytically be determined by Theis's equation (Equation 2.1). Theis's method is applicable on the situation depicted in 2.2b; a constant rate pumping test in a fully penetrating well connected to a confined single layer aquifer (Kruseman & de Ridder, 2000). The analytical solution is easily applicable and ideally suitable as a first geohydrological parameter indication.

$$s = \frac{Q}{4\pi K D} \exp1(u) \quad (2.1)$$

$$u = \frac{r^2 S}{4 K D t} \quad (2.2)$$

Where s (m) is the drawdown at distance r (m) from the well, Q (m^3) is the constant well discharge , $K D$ (m^2/d) is the aquifer transmissivity ($K D = T$), S (-) is the aquifer storativity, t (d) is the time measured from the start of pumping and $\exp1$ is the exponential integral. The fieldwork drawdown measurements of this research are limited to in-well measurements only. For this research purposes the distance r in the Theis's equation is assumed to be the length of the well radius (0.0635 m). Theis's method is applicable for the time of pumping as well as the recovery process, as mentioned in the script below.

```
252
253 def drawdown(t, T, S):
254     s = Qo / (4 * np.pi * T) * exp1(ro ** 2 * S / (4 * T * t))
255     s[t > toff] -= Qo / (4 * np.pi * T) * exp1(ro ** 2 * S / (4 * T * (t[t>toff] -
256                                         toff)))
257
258     return s
```

TTim Analytical Element modelling

TTim is a computer program based on analytic elements and designed for the analysis of groundwater flow in one or more layers. The program is characterized by its simplistic model configuration. Multiple elements (and elements types) can be added one-by-one to specific predefined model layers. By the use of TTim (compared to the analytical Theis's method for example) it is possible to take additional well characteristics into account. Groundwater heads can be determined inside the well and the model optionally accounts for borehole storage and potential well skin resistance. Moreover, TTim is of particular functionality for the modelling of transient groundwater flow (bron??). Groundwater well discharge can be switched on and off easily and numerous times. Making TTim not only a program suitable for the simulation of a single pumping test(pumping and recovery), long duration use of the well can also be simulated.

The analysis of this fieldwork data is designed by the use of the TTim Model3D configuration. Although multiple elements can be part of the model, the inclusion of a single well (element) is sufficient in this case. Dependent on model design (2.2) the well (analytical element) is connected to one or more model layers. In the TTim fieldwork data analysis the model top layer configuration is tagged as confined with a true phreatic top (based on observed initial groundwater tables). By the use of this specific set-up the top layer storage coefficient (S) is a phreatic storage (S_y). Multiplying this value with the aquifer thickness is therefore no longer needed. This is moreover not an issue due to the general model simulation in which each model layer is defined with a 1 m thickness. The result is a simulation where derived hydraulic conductivities (K) can be interpreted as transmissivities (T) and the storage is expressed as the layer storage coefficient (S). This is predominantly done to directly derive T and S values. At the same time the approach naturally corrects for the unknown thickness of the deepest well penetrated soil layer (information on bottom soil layer depth absent in the borehole log-sheets of A).

MODFLOW

The subsequent scenario modelling (chapter 3) of this research is applied in USGS's modular model MODFLOW, the international standard in groundwater simulation (bron??). Regarding fieldwork data analysis MODFLOW is not used in the optimization process of geohydrological parameters. Optimal parameters (found by the use of TTim) are only implemented in corresponding MODFLOW simulations as a reference to validate the TTim results.

2.1.3. Optimization functions

Generated fieldwork pumping test data (section 2.4) is used as an input for the derivation of local geohydrological parameter values. The most likely applicable T and S values are determined by correlating the analytical solutions and/or TTim models to the gathered data. In this research optimization process two fit

294 functions are applied.

295

296 Fmin-RMSE optimization

297 Deviations between fieldwork data and modelled drawdown curves can be expressed by the RMSE-value,
 298 equation 2.3 (bron??). To minimize this error, and difference between modelled and fieldwork data, the
 299 Fmin function is applied (scipy.optimize package). Result is the determination of optimal T and S values
 300 (and optionally values for boreholes storage and well skin resistance) approximately representing the local
 301 circumstances. An example of Fmin-RMSE optimization python coding is depicted below. The example
 302 contains an optimization of five parameters (T and S values for two layers and an optimal well skin resis-
 303 tance).

304



$$RMSE = \sqrt{\frac{\sum (s_{mod} - s_{field})^2}{N}} \quad (2.3)$$

305 Where s_{mod} is the modelled drawdown (m), s_{field} is the fieldwork measured drawdown (m) and N is the
 306 number of data points.

307

```
308 def optimTTim_Qvar(params, t, meas):
309     kaq = np.zeros(2)
310     Saq = np.zeros(2)
311     kaq[0] = params[0]
312     kaq[1] = params[1]
313     Saq[0] = params[2]
314     Saq[1] = params[3]
315     res = params[4]
316     s = drawdownTTim_Qvar(t, kaq, Saq, res)
317     error = np.sqrt(np.mean((s-meas)**2))
318
319     return error
320
321 xopt = fmin(optimTTim_Qvar, x0=[10, 10, .01, .001, 0.1], args=(to[mask], do[mask]),
322               xtol=1e-4)
```

324 Calibration function

325 Besides the application of minimizing the RMSE it is also possible to derive optimal geohydrological pa-
 326 rameter values by the Calibrate function of TTIm. This optimization function is applied in the research to
 327 improve the parameter value derivation robustness. In the python coding below, an example TTIm Calibrate
 328 function is given. Content-wise it is the same example mentioned in the Fmin-RMSE optimization above.

329

```
330 cal = Calibrate(mlc)
331 cal.parameter(name='kaq0', layer=0, initial=10, pmin=0)
332 cal.parameter(name='kaq1', layer=1, initial=10, pmin=0)
333 cal.parameter(name='Saq0', layer=0, initial=.01, pmin=0, pmax=0.3)
334 cal.parameter(name='Saq1', layer=1, initial=.001, pmin=0, pmax=0.3)
335 cal.parameter(name='res', par=wc.res, initial=0.1)
336 cal.series(name='obs3', x=ro, y=0, layer=[0,1], t=to[mask], h=-do[mask])
337 cal.fit()
```

340 These optimization techniques require initial parameter conditions. Possibly there is more than one op-
 341 timal solution applicable. Making the outcome of the data analysis dependent on the arbitrary chosen
 342 starting values. Northern Ghana T and S values are commonly low (Owusu et al, 2017). In this research
 343 the following initial conditions are applied: kaq_0 is 10 (m/d), kaq_1 is 10 (m/d), Saq_0 is 0.01 (-), Saq_1 is 0.001
 344 (-) and well resistance is 0.1 (d). The in-field measured well radius is used as the (initial) borehole storage:
 345 0.0635 (m). To avoid the occurrence of unlikely parameter values, boundary conditions are applied. The
 346 emergence of negative parameter values is prevented by setting the minimum parameter bound equal to
 347 zero. While unnaturally high storativity values are ignored by upper bounds of 0.3 (-).

2.2. From fieldwork data to T & S values

Above mentioned model simplifications and methods in data analysis are applied on the research locations: Bingo, Nungo, Nyong Nayili, Janga and Ziong. In the TTIm analys an additional distinction is made by optionally applied optimizations in actual and/or optimal borehole storage and well resistance. A complete overview of all simulations applied can be found in appendix C. Most important outcomes of these analysis are for each research location further elaborated below.

2.2.1. Location: Bingo

Site inspection

Sloping landscape, some rocks at surface. Area dominated by bush fires, charred vegetation abundant, agricultural field not ready for use. Although Volta river far (on map), no river, water flow or ponds seen in direct surroundings. Wet season floodings caused by rain and 'popping up' out ground, labelled as height (1-2m) and disappears in days. At walking distance from nearest community. Steel lid, no tube perforations above surface level.

361

Measurement quality

Start delayed due to malfunctioning power converter. Tangled rope: Position lowest diver undesirably high and hand measurements not completely possible, result: big gap in data. Recovery test started at an early stage.

366

Fit analysis

Data point are missing. Total drawdown unknown from a certain moment in time. The analytical (Theis) solution is not capable of correcting for this measurement  lack. This is most definitely not the case for the data analysed by the use of TTIm. The use of both parameter optimization methods are capable of correcting for the lack of data. Both optimizations find optimal parameter values at which drawdown curve exceeds lowest measured groundwater levels. By this example it is shown it is not by definition required to feature complete drawdown curves during parameter determination. Even with incomplete drawdown time series it is possible to obtain reasonable fits. Complete overview of all the optimizations applied (13x) can be found in appendix.. tell about the wobbly curve, due to measured fluctuation in discharge.

376

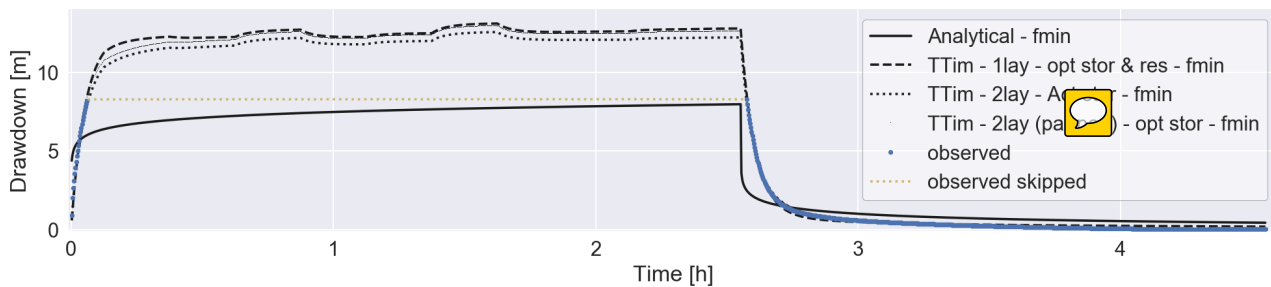


Figure 2.3: Bingo - multi-layer best fits

Table 2.1: Bingo - overview best fit parameters

	Method	Stor [m]	Res [d]	T1	T2 [m^2/d]	S1	S2 [-]	RMSE [m]
Analytical	fmin	-	-	10.83	-	2.0e-04	-	0.798133
1 lay	fmin	0.0647	5.6e-02	26.23		6.6e-03	-	0.16 
2 lay	fmin	0.0635	-	2.8e-04	08.25	3.0e-03	2.1e-06	0.10 
2 lay (pp)	fmin	0.0597	-	8.6e-04	07.44	7.1e-03	6.3e-06	0.078188

377 Final remark korte uitleg welke fit nou het beste is? en waarom.

2.2.2. Location: Nungo

Site inspection

380 **Measurement quality**

381 **Fit analysis**

382 **Final remark**

383 **2.2.3. Location: Nyong Nayili**

384 **Site inspection**

385 **Measurement quality** data skip applied. **Fit analysis**

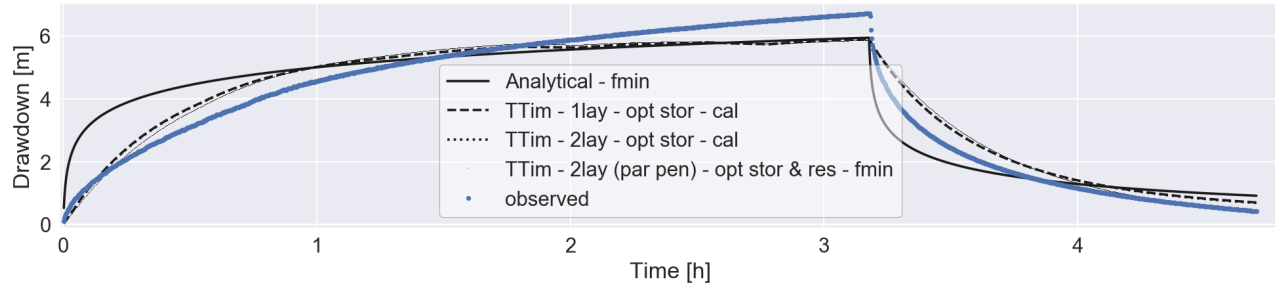


Figure 2.4: Nyong Nayili - multi-layer best fits

Table 2.2: Nyong Nayili - overview best fit parameters

	Method	Stor [m]	Res [d]	T1	T2 [m²/d]	S1	S2 [-]	RMSE [m]
Analytical	fmin	-	-	06.00	-	3.0e-01	-	0.751699
1 lay	cal	0.2419	-	13.35	-	7.8e-05	-	0.457474
2 lay	cal	0.2436	-	06.95	06.98	4.6e-06	3.6e-05	0.456774
2 lay (pp)	fmin	0.2659	1.7e-02	1.7e-04	28.61	1.1e-02	4.4e-06	0.450121

386 **Final remark**

387 **2.2.4. Location: Janga (1/2)**

388 **Site inspection**

389 **Measurement quality**

390 **Fit analysis**

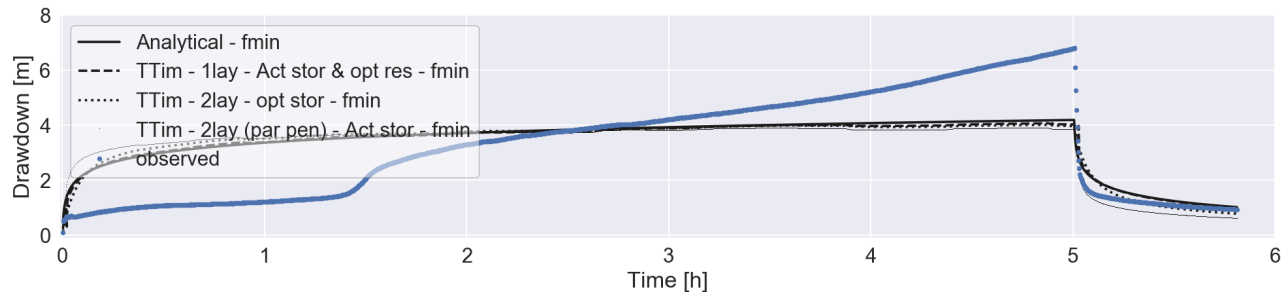


Figure 2.5: Janga first attempt - multi-layer best fits

Table 2.3: Janga first attempt - overview best fit parameters

	Method	Stor [m]	Res [d]	T1	T2 [m²/d]	S1	S2 [-]	RMSE [m]
Analytical	fmin	-	-	08.84	-	3.0e-01	-	1.338604
1 lay	fmin	0.0635	-9.7e-03	09.09	-	1.6e-02	-	1.382181
2 lay	fmin	0.1287	-	12.48	1.3e-04	1.9e-02	1.1e-08	1.444546
2 lay (pp)	fmin	0.0635	-	9.1e-05	15.19	4.3e-08	3.1e-03	1.530254

391 **Final remark**

392 **2.2.5. Location: Janga (2/2)**

393 **Measurement quality**

394 **Fit analysis**

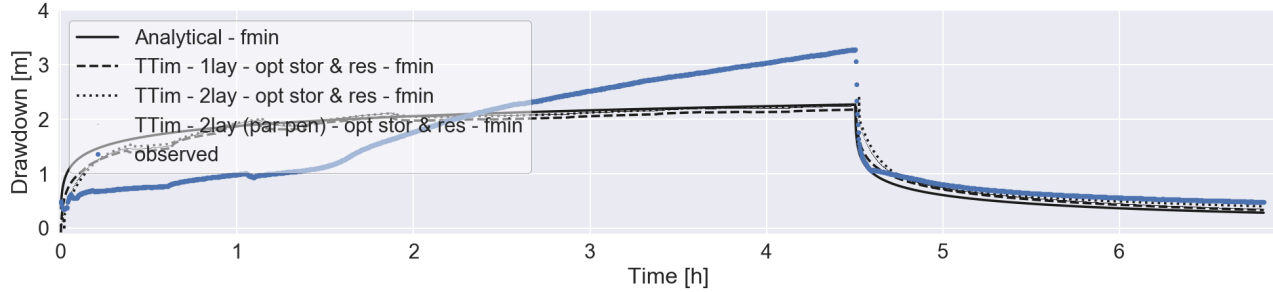


Figure 2.6: Janga second attempt - multi-layer best fits

Table 2.4: Janga second attempt - overview best fit parameters

	Method	Stor [m]	Res [d]	T1	T2 [m ² /d]	S1	S2 [-]	RMSE [m]
Analytical	fmin	-	-	15.97	-	3.0e-01	-	0.570855
1 lay	fmin	5.4e-07	-9.7e-03	13.54	-	1.9e-02	-	0.550853
2 lay	fmin	0.2228	-2.2e-02	02.05	08.13	2.1e-02	4.1e-04	0.544680
2 lay (pp)	fmin	0.2005	-3.1e-02	06.59	00.86	9.4e-05	2.1e-03	0.544540

395 **Final remark**

396 **2.2.6. Location: Ziong (monitoring)**

397 **Site inspection**

398 **Measurement quality** multi day use. Anaytical solution not applied. **Fit analysis**

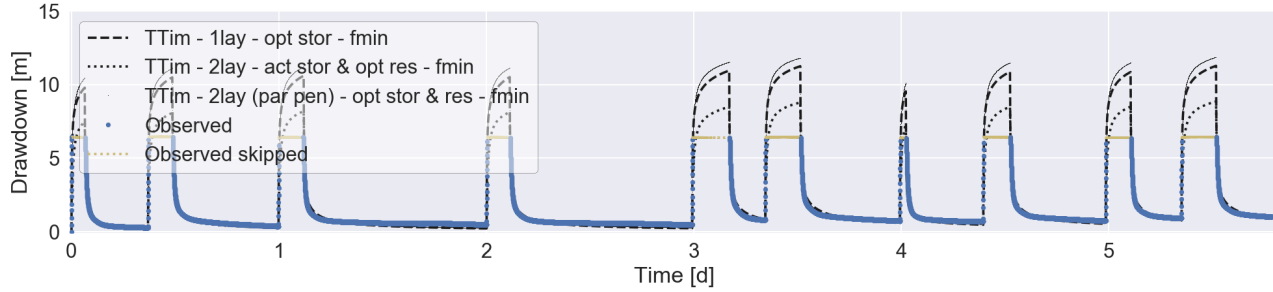


Figure 2.7: Ziong - multi-layer best fits

Table 2.5: Ziong - overview best fit parameters

	Method	Stor [m]	Res [d]	T1	T2 [m ² /d]	S1	S2 [-]	RMSE [m]
1 lay	fmin	0.0382	-	01.76	-	1.1e-03	-	0.254574
2 lay	fmin	0.0635	-0.05	00.38	01.05	2.9e-02	1.2e-03	0.240162
2 lay (pp)	fmin	0.0147	-0.08	00.23	00.78	2.6e-02	1.3e-03	0.243108

399 **Final remark**

400 **2.3. Theoretical validation**

401 **Soil analysis**

402 **VES analysis**

403 2.4. Fieldwork results

404 summary of the main results Recommendations for further investigation if applicable.

405 Waardes komen overeen (zelfde range/ordegrootte) met theorie. zoek dit even na

406
407 Er is geen duidelijk onderscheid of 1, 2 dan wel 3 laags (partially penetrating) beter dan wel slechter scoort.
408 dus alle schematische gelaagde bodemoppbouw mogelijk.

409
410 bespreek hier de tekortkoming van het meten in de well zelf als enige. Werkt gewoon niet heel fijn of
411 nauwkeurig. Voor indicatie wel goed.

412
413 vertel over het resultaat van de twee vormen van analyse. fmin versus calibration function. Toch een ver-
414 schil in algoritme (numerieke solver). Maar resultaten beide slechts tot op zekere hoogte nauwkeurig. Maar
415 dit zal eerder komen door de metingen zelf (in borehole) en de omstansigheden van northern Ghana.

416
417 does not happen to often. but if T or S values not in right 'order', it is always assumed highest T values
418 in layer under confining layer (not in lowest layer). based on the known soil type of this layer in borehole
419 logsheet (appendix..).

420
421 schrijf appendix over de lambda bepaling.

3

422

423

Model scenarios

424 scenario's

425 **3.1. Scenarios**

426 **3.2. Test criteria**

427 **3.3. Run**

428 **3.4. Results & Conclusions**

4

429

430

(Financial) yields - upscaling

431 kostenplaatje

432 **4.1. inhoud**

5

433

434

435 Results short outcome of upscaling. Does it work?

Conclusions

6

436

437

Discussion & Recommendations

438 good, bad, advice further research

Bibliography

Appendices

441

A

442

Original Borehole Logsheets

443 In the first half of the year 2016 Conservation Alliance (CA) commissioned the construction of multiple
444 boreholes in northern Ghana. The boreholes subjected in this research (five locations, visualized in 2.1) are
445 all part of this operation. Valuable information is gained with respect to local soil stratification, during
446 borehole construction. Information is preserved in the original borehole log-sheets, which can be found
447 in this appendix. Besides the local soil stratification, these log-sheets contain information on individual
448 applied well structures. A depth dependent distinction is made in plain versus screened well skin. In terms
449 of content these borehole log-sheets are used as a starting point in the theoretical model determination
450 (section 2.1).

		CONSERVATION ALLIANCE- THE PAVE PROJECT				BH status:	Successful	✓			
						Dry					
		BOREHOLE LOG SHEET									
Community		Bingo	District	Talensi	Borehole ID	BH B1					
Coordinates - Latitude (N) :		Longitude (W)									
Drilling contractor		Drill rig				Method	ROTARY AIR				
Drilling start date		6-8-2016	Compl. date	6-8-2016	Operator						
TEST PUMPING		Date:				Conductivity	us/cm	Top of screen *	0 m		
Dynamic WL *		m	Pump type				Total Iron	mg/l	Static WL *	m	
Static WL *		m	Pumping rate (Q)				m³/h	Manganese	mg/l	Potential drawdown	m
Drawdown (s)		m	Duration				h	Nitrate	mg/l	Potential yield	25 l/min
* Levels to ground level datum		Specific capacity (Q/s)			m³/h/m		Fluoride	mg/l	Depth of borehole *	48 m	
BIT SIZE & TYPE	Temporary Casing	SCALE	PROFILE		TIME/DEPTH M/MIN	WATER ZONES CUMULATIVE Q (l/min)	WELL DIAGRAM				
10"			Light brown clay								
Clay cutter											
6.5" hammer bit			Highly weathered light brown sandstone mixed with shaly materials								
			5								
			10								
			15								
			20								
			25								
			30								
			35								
			40								
			45								
50											
Gravel for gravel pack		48	LM	Remarks and stoppages:							
Screen Length		30	LM								
Casing length		18	LM								
Installation of grout seal		M	M								
Cleaning & development		2	HRS	Prepared by:							
Centralisers fitted			No								
Safety cap fitted		/	No	Approved:							
Backfill aband. BH			/								
Cement for grout			KG								
Platform construction date											
Distance from last BH			KM								

		CONSERVATION ALLIANCE- THE PAVE PROJECT				BH status:		Successful		✓	
		BOREHOLE LOG SHEET				Dry					
Community		Nungo		District	Talensi	Borehole ID	BH N100				
Coordinates - Latitude (N) :		Longitude (W)									
Drilling contractor				Drill rig			Method	ROTARY AIR			
Drilling start date		6-8-2016		Compl. date	6-8-2016	Operator	Kwaku				
TEST PUMPING		Date:			Conductivity	us/cm	Top of screen *	0	m		
Dynamic WL *		m	Pump type		Total Iron	mg/l	Static WL *		m		
Static WL *		m	Pumping rate (Q)	m³/h	Manganese	mg/l	Potential drawdown		m		
Drawdown (s)		m	Duration	h	Nitrate	mg/l	Potential yield	80	l/min		
* Levels to ground level datum		Specific capacity (Q/s)		m³/h/m	Fluoride	mg/l	Depth of borehole *	42	m		
BIT SIZE & TYPE	Temporary Casing	SCALE	PROFILE		TIME/DEPTH M/MIN	WATER ZONES CUMULATIVE Q (l/min)	WELL DIAGRAM				
10"	Clay cutter		Highly weathered light brown sandstone								
										5	
										10	
										15	
										20	
										25	
										30	
										35	
										40	
										45	
										50	
6.5" hammer bit			Moderately weathered light grey sandstone mixed with shaly materials (at 18m, 21-24m)								
										18m PVC Plain	
										20	
										25	
										30	
										35	
										40	
										45	
										50	
Gravel for gravel pack			42	LM	Remarks and stoppages:						
Screen Length			36	LM							
Casing length			6	LM							
Installation of grout seal			M	M							
Cleaning & development			2	HRS	Prepared by:						
Centralisers fitted			No								
Safety cap fitted			/								
Backfill aband. BH			No	/							
Cement for grout			KG								
Platform construction date											
Distance from last BH			KM								

		CONSERVATION ALLIANCE- THE PAVE PROJECT				BH status:	Successful	✓
						Dry		
BOREHOLE LOG SHEET								
Community	Nyong Nayili	District	Karaga	Borehole ID	BH NN1			
Coordinates - Latitude (N) : Longitude (W)								
Drilling contractor		Drill rig		Method	ROTARY AIR			
Drilling start date	31/05/2016	Compl. date	31/05/2016	Operator	Kwaku			
TEST PUMPING		Date:		Conductivity	us/cm	Top of screen *	0	m
Dynamic WL *	m	Pump type		Total Iron	mg/l	Static WL *		m
Static WL *	m	Pumping rate (Q)		m³/h	Manganese	mg/l	Potential drawdown	m
Drawdown (s)	m	Duration		h	Nitrate	mg/l	Potential yield	
* Levels to ground level datum		Specific capacity (Q/s)		m³/h/m	Fluoride	mg/l	Depth of borehole *	54 m
BIT SIZE & TYPE	Temporary Casing	PROFILE SCALE	TIME/DEPTH M/MIN	WATER ZONES CUMULATIVE Q (l/min)	WELL DIAGRAM			
10"								
Clay cutter		Clay						
		5						
		10						
		15						
		20						
		25						
		30						
		35						
		40						
		45						
		50						
		55						
Gravel for gravel pack	Yes	54	LM	Remarks and stoppages:				
Screen Length		33	LM					
Casing length		21	LM					
Installation of grout seal		M	M					
Cleaning & development		2	HRS	Prepared by:				
Centralisers fitted		No						
Safety cap fitted	/	No	Approved:					
Backfill aband. BH	Yes	/						
Cement for grout		KG						
Platform construction date								
Distance from last BH		KM						

		CONSERVATION ALLIANCE- THE PAVE PROJECT				BH status:		Successful		✓
		BOREHOLE LOG SHEET				Dry				
Community	Janga 1	District	West Mamprusi	Borehole ID	BH J1					
Coordinates - Latitude (N) :	0°iu	Longitude (W)								
Drilling contractor		Drill rig				Method	ROTARY AIR			
Drilling start date	6-3-2016	Compl. date	6-3-2016			Operator	Kwaku			
TEST PUMPING		Date:			Conductivity	us/cm	Top of screen *	0	m	
Dynamic WL *	m	Pump type			Total Iron	mg/l	Static WL *		m	
Static WL *	m	Pumping rate (Q)			Manganese	mg/l	Potential drawdown		m	
Drawdown (s)	m	Duration			h	Nitrate	mg/l	Potential yield	35 l/min	
* Levels to ground level datum		Specific capacity (Q/s)			m³/h/m	Fluoride	mg/l	Depth of borehole *	48 m	
BIT SIZE & TYPE	Temporary CASING SCALE	PROFILE			TIME/DEPTH M/MIN	WATER ZONES CUMULATIVE Q (l/min)	WELL DIAGRAM			
10" Clay cutter										
		5	Highly weathered light brown sandstone (Very loose formation)							5
		10								10
		15								15
		20								20
		25								25
		30								30
		35								35
		40								40
		45								45
		50								50
Gravel for gravel pack		48	LM	Remarks and stoppages:						
Screen Length		48	LM							
Casing length			LM							
Installation of grout seal			M							
Cleaning & development		2	HRS	Prepared by:						
Centralisers fitted			No							
Safety cap fitted		/	No	Approved:						
Backfill aband. BH			/							
Cement for grout			KG							
Platform construction date			KM							
Distance from last BH										

		CONSERVATION ALLIANCE- THE PAVE PROJECT				BH status:	Successful	✓		
						Dry				
BOREHOLE LOG SHEET										
Community	Ziong	District	Savelugu Nanton	Borehole ID	BH Z1					
Coordinates - Latitude (N) : Longitude (W)										
Drilling contractor		Drill rig		Method	ROTARY AIR					
Drilling start date	27/05/2016	Compl. date	27/05/2016	Operator						
TEST PUMPING		Date:		Conductivity	us/cm	Top of screen *	0	m		
Dynamic WL *	m	Pump type		Total Iron	mg/l	Static WL *		m		
Static WL *	m	Pumping rate (Q)		m³/h	Manganese	mg/l	Potential drawdown	m		
Drawdown (s)	m	Duration		h	Nitrate	mg/l	Potential yield	25 l/min		
* Levels to ground level datum		Specific capacity (Q/s)		m³/h/m	Fluoride	mg/l	Depth of borehole *	48 m		
BIT SIZE & TYPE	Temporary Casing	PROFILE SCALE	TIME/DEPTH M/MIN	WATER ZONES CUMULATIVE Q (l/min)	WELL DIAGRAM					
10"										
Clay cutter										
6.5" hammer bit		Reddish brown laterite								
		5								3m PVC Screen
		10								5
		15								10
		20								15
		25								20
		30								25
		35								30
		40								35
		45								40
50								45		
Highly weathered light brown sandstone mixed with shaly materials										
Moderately weathered brownish sandstone										
Gravel for gravel pack	48	LM	Remarks and stoppages:							
Screen Length	36	LM								
Casing length	12	LM								
Installation of grout seal	M	M								
Cleaning & development	2	HRS	Prepared by:							
Centralisers fitted		No								
Safety cap fitted	/	No	Approved:							
Backfill aband. BH	Yes	/								
Cement for grout		No								
Platform construction date		KG								
Distance from last BH		KM								

B

456

457

Fieldwork set-up

458 The northern Ghana in-field geohydrological data collection would not have been possible without the in-
459 terference of Conservation Alliance (CA). Spread over the Upper East and Northern Region the NGO holds
460 multiple PIT locations. Five locations, visible in figure 2.1, are appointed as measurement locations for the
461 purposes of this research. Besides the research locations, CA provided transport, an interpreter and pump-
462 ing test equipment. The section below contains detailed information on the equipment applied. Moreover,
463 it describes the general fieldwork pumping test / monitoring set-up. The section concludes with fieldwork
464 fact-sheets, containing the collected data for each individual location.

465 **B.1. Equipment**

466 The applied in-field pumping tests are executed with a same set of equipment. The paragraph below con-
467 tains a detailed description of the most important tools. In this case a distinction has been made between
468 the equipment for the pumping tests and the actual groundwater measurements. Moreover small equip-
469 ment as pliers, screwdrivers, gloves and robes are ignored. Purposes and use of these tools are taken for
470 granted.

471

472 **Pumping test**

- 473 • Pump: Pedrollo 4" submersible pump; Type 4SR4/18

474 A 2 HP pump, for example usable for the supply of water to irrigation fields. While pumping the water
475 should preferably not exceed 35 °C and should not contain too many particles; no more than 150
476 g/m³. The pump can be submerged in water up to 100 meters. Installed in the right way, the pump
477 can deliver 20-100 l/min with an head difference of 112-45 m. More specific information regarding
478 the pump can be found on the Pedrollo webpage.



Figure B.1: Comparable example of the fieldwork submersible pump
(source: <https://www.pedrollo.com/en/4sr-4-submersible-pumps/150>)

479 • Generator & power converter: Kipor diesel generator - 5 kVA

480 A mobile generator has been used as a pump power source. The Kipor generator is a relatively small
 481 model, easy to handle and meets the pump requirements by the use of the 230 V connection. A power
 482 converter is placed between generator and pump to manually switch on and off the pump. To facilitate
 483 a flawless transfer between generator and pump one should be aware the cables and connections
 484 towards the pump should be waterproof. Moreover these power cables should be of a decent length
 485 to allow the pump to submerge.



Figure B.2: Comparable example of the fieldwork generator

(source: <https://www.kipor-power.eu/winkel/kipor-kde6700t-diesel-generator-5-kva/>)

486 • Hose:

487 As a transport line towards the location of discharge a flexible water hose has been attached to the
 488 pump. The hose has been manufactured in Polyethylene, has an external diameter of $1\frac{1}{4}$ " and is
 489 approximately 100 m long.



Figure B.3: Actual fieldwork hose & bucket

490 • Bucket:

491 As a rough estimation for discharge an plastic bucket has been used. This oversized measuring cup
 492 stores volumes up to 50 l and contains 5 l level indicators.

493 **GWT measurements**

494 • Pressure sensor data loggers:

495 - Van Essen; TD-Diver Type DI801 (2x) & Baro-Diver Type DI800 (1x):

496 TD- and Baro-Divers are applied for the measuring and recording of time dependent fluctuations in
 497 (ground)water levels, atmospheric pressures and temperatures. The TD-Divers can record a water
 498 column up to 10 m. Baro-Divers can be used to measure atmospheric pressures and shallow water
 499 levels, approximately up to a range of 0.9 m. Based on the internal memory these devices can store

500 up to 72.000 measurements per parameter. Measurement logging can be programmed by the use
 501 of a USB-Unit and the Diver-Office software. With a battery life of 10 years, long and/or short term
 502 measurements can be applied with a sample interval of 0.5 seconds to 99 hours. Moreover the sample
 503 interval can be linear or logarithmic.



Figure B.4: Comparable examples of Van Essen TD- & Baro-Divers
 (source: <https://www.vanessen.com/images/PDFs/TD-Diver-DI8xx-ProductManual-nl.pdf>)

504 - In-Situ; RuggedTROLL100 (2x) & BaroTROLL (1x):

505 Rugged TROLL 100 and BaroTROLL divers are applied for the measuring and recording of time depen-
 506 dent fluctuations in (ground)water levels, atmospheric pressures and temperatures. The RuggedTROLL100
 507 divers function in a pressure range up to 9 m water column. BaroTROLL divers can be used for the
 508 measurement of atmospheric pressures, up to 1 bar. The internal memory of 2.0 MB accommodates
 509 the storage of 120.000 data records. A record contains a set of three items; date & time, pressure and
 510 temperature. The internal battery has a lifetime of approximately 10 years. By the use of the Rugged
 511 TROLL docking-station and the Win-Situ 5 software, linear logging can be programmed. Fastest log-
 512 ging rate is 1 log per second for the Rugged TROLL 100 divers and 1 log per minute for the BaroTROLL
 513 divers. Optionally it is possible to display the pressure in units of Psi, Bar, Pascal or mH₂O.



Figure B.5: Comparable examples of In-Situ TD- & Baro-Divers
 (source: <https://in-situ.com/product-category/water-level-monitoring/level-temp-data-loggers/>)

514 • Hand measurement device: Heron water tape

515 The water tape is applied to hand measure static water levels and verify drawdown water levels during
 516 the pumping tests. The water tape has a length of 300 ft (100 m). A water level sensing probe is
 517 attached to the tail of the tape. Probe water contact results in an instant auditory signal, after which
 518 the depth can be determined by eye. Product specifications can be found on the Heron webpage.

519 **B.2. General measurement structure**

520 This section accommodates multiple key aspects in the test set-up. By the implementation of this thought-
 521 out pumping test and measurement set-up an optimal test result is pursued. Moreover it accommodates



Figure B.6: Comparable example of the fieldwork water tape
(source: <https://envirotechonline.com/water-level-interface-meters/the-heron-water-tape.html>)

522 information on fieldwork reproduction.

523 **Pump installation**

524 Based on the log sheets the original (2016) site-specific borehole depths are known in advance. Due to the
525 accumulation of sedimentation the borehole depth decreases over time. To prevent pump damage and
526 make sure proper functioning is maintained, the actual borehole depths are measured before the pump-
527 ing tests. Outcome of the measurements are taken into account for each individual test set-up. To prevent
528 excessive spread of soil particles the submersible pump is positioned at least 5 meters above the measured
529 bottom. In practice this resulted in a pump suction depth of approximately 35 m for every individual pump-
530 ing test.

531 **Discharge (measurement)**

532 A single 100 m hose is directly connected to the outlet of the submersible pump. Based on the pump position
533 (deep inside borehole), a length of circa 60 m is still present for the horizontal displacement of water.
534 At this distance (relative to the borehole) water is discharged on the surface.
535 The head of the hose is equipped with a nozzle to roughly regulate the discharge rate. By the use of this nozzle,
536 discharge rates in the range of 50-75 m³/d are obtained during the pumping tests. Rates are measured
537 by the use of a 50 l bucket. Starting at the moment of pump operation, the duration of filling is measured
538 twice every 15 minutes. The average is used to calculate the time dependent discharge rates. More detailed
539 discharge information can be found in the site-specific fact-sheets below.

540 **GWT measurement**

541 Drawdowns due to pumping tests are preferably measured in multiple piezometers located at a certain
542 known horizontal distance from the discharge well (Kruseman & de Ridder, 2000). In the northern Ghana
543 surroundings, close range monitoring options are absent. Due to a lack of time and/or resources these fa-
544 cilities cannot be arranged either. Moreover, the implementation of such facilities do not match research
545 nature. Aim of this research is to collect fieldwork data by the use of minimal resources. The local absence of
546 abundant measurement options strengthens this approach. In this research pumping test GWT drawdowns
547 are measured in the discharge well only.

548 A water tape (hand equipment) is used, first of all to determine the initial (static) GWT. Subsequently the de-
549 vice is applied as a real time indicator of drawdown. During the pumping test multiple hand measurements
550 are applied at randomly picked moments to monitor test progress. Gathered data functions as verification
551 and back-up of the pressure sensors, which are normative.

552 Two types of divers (different brands) are used as basic GWT measurement devices. Specifications show
553 these divers can respectively measure pressures up to 10 m (Van Essen) and 9 m (In-Situ) water column
554 (bron.). The northern Ghana regional subsurface is characterized as highly heterogeneous. The pumping
555 test GWT drawdown order of magnitude is therefore unpredictable. To prevent the occurrence of missing

556 drawdown data, the single borehole accommodates multiple divers at ascending depths. The water column
 557 between the initial static water table and pump position is preferably filled with about four divers, with a
 558 mutual distance that meets the divers range specifications. To make sure the divers stay in position they are
 559 leashed to a rope which runs from well top to pump. This measurement set-up forms a robust network for
 560 the collection of drawdown data.

561 Practical circumstance can however cause the application of a more simplified set-up. One can think of a
 562 situation in which the pump is already installed and/or will not be removed at the end of the pumping test.
 563 Rope attachment of the divers to the pump is in this case no longer possible. Adverse effect of the sim-
 564 plified set-up is a data collection which is more vulnerable. To prevent the occurrence of undesired diver
 565 movement a minimum distance of 5-10 m between pump and lowest diver is implemented in the simplified
 566 set-up. A complete overview of the borehole measurement set-up (desired and simplified) can be found in
 567 figure B.7.

568

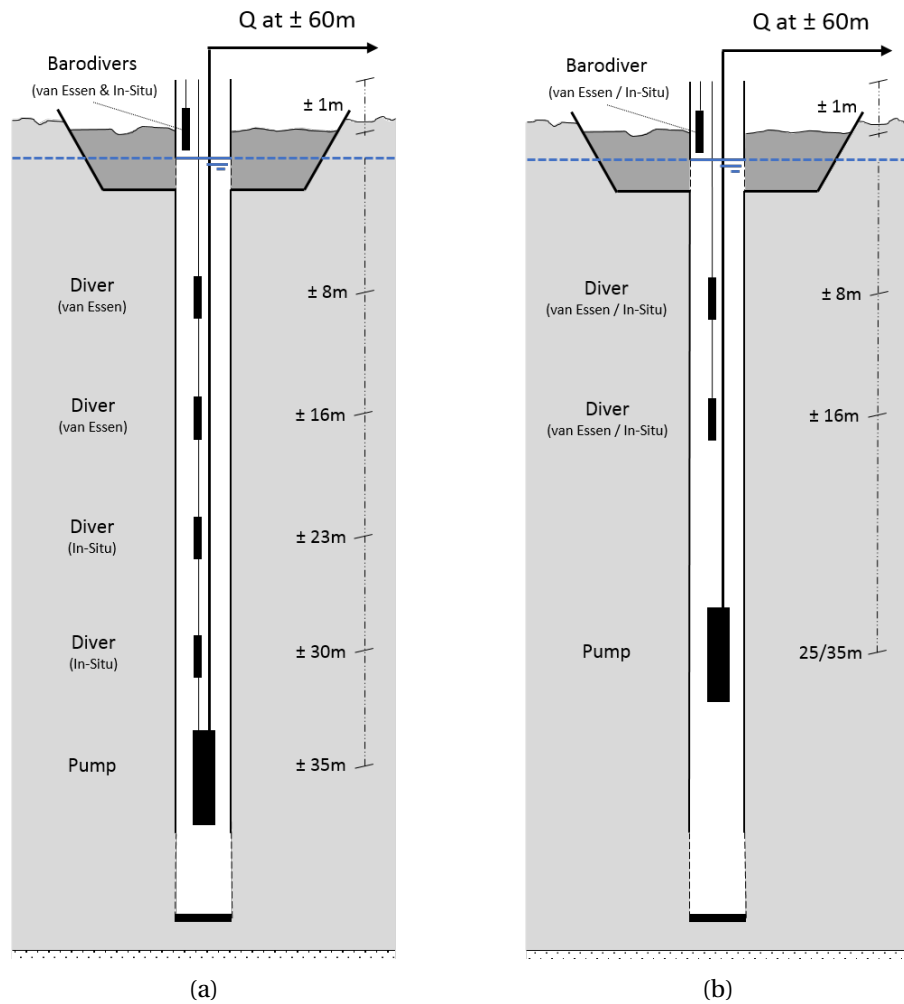


Figure B.7: Fieldwork (measurement) set-up (a) general, (b) simplified

569 Besides the divers the measurement set-up also accommodates two Baro-divers (van Essen & In-Situ), posi-
 570 tioned in the borehole top section. Drawdown is by definition expressed as time dependent GWT reductions
 571 relative to the initial status (bron.). Short term atmospheric fluctuations in pressure are compared to the
 572 water pressures negligible small. Nonetheless these minor atmospheric influences are also included in the
 573 data collection. The inclusion of these Baro-diver measurements increases measurement accuracy, espe-
 574 cially with respect to the multi-day system monitoring.

575 The exact start of pump operation could not be determined in advance. To avoid unnecessary risks in miss-
 576 ing out on the collection of drawdown data, all pressure sensors are programmed to start logging well in
 577 time (08:00:00, local time, at pumping test days). All divers are set to log with a similar linear interval of

578 10 seconds. Only exception is the In-Situ BaroTROLL, which is programmed to linear log at its minimum
579 sample interval; once a minute.

580 **B.3. Site-specific measurement results**

581 In consultation with Conservation Alliance (CA), a total of five pumping tests are applied in boreholes lo-
582 cated at Bingo, Nungo, Nyong Nayili and Janga. By the use of a fifth borehole, location Ziong, the day-to-day
583 PIT system-use is monitored for a week. All tests are applied in November-December 2017, shortly after the
584 transition from wet to dry season. Geohydrological data is gathered by the application of the general pump-
585 ing test set-up (as described above) at the location Nungo, Nyong Nayili and Janga. The simplified set-up is
586 applied at the location Bingo and Ziong. Outcome of the tests are widespread. Detailed site-specific results
587 are displayed in the fact-sheet figures below (Figures B.8 - B.13).

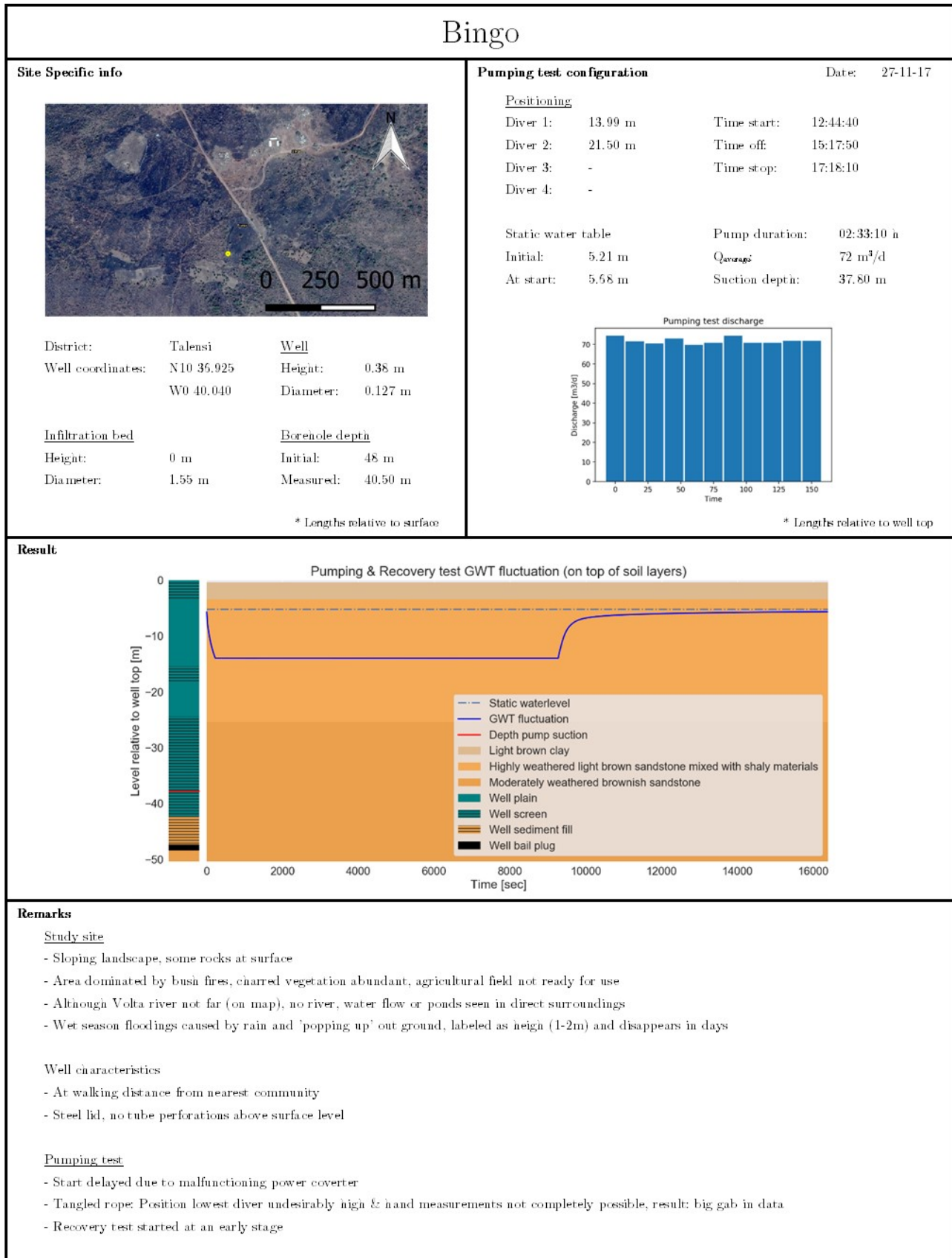


Figure B.8: Fieldwork fact-sheet: Bingo

Nungo		
Site Specific info	Pumping test configuration	Date: 28-11-17
 <p>District: Tafensi Well</p> <p>Well coordinates: N10 33.419 Height: 0.51 m W0 38.990 Diameter: 0.127 m</p>	<u>Positioning</u> Diver 1: 9.05 m Time start: 09:45:00 Diver 2: 17.90 m Time off: 11:00:00 Diver 3: 26.05 m Time stop: 11:15:00 Diver 4: -	
	<u>Static water table</u> Initial: 3.02 m Pump duration: 01:15:00 h At start: 3.00 m Q _{average} : < 5 m ³ /d Suction depth: 31.20 m	
		Pumping test aborted
<u>Infiltration bed</u> Height: -0.35 m Initial: 42 m Diameter: 1.50 m Measured: 9.80 m		
		* Lengths relative to surface
		* Lengths relative to well top
Result -		
		Pumping test aborted
Remarks		
<u>Study site</u> - Mildly sloped till flat landscape - Vegetation abundant, agricultural field present but not ready for use - Volta river in close range (approximately 400 m) - Wet season floodings caused by riverbank overtopping; labeled as extreme (>3m) and constant; duration as long as wetseason		
<u>Well characteristics</u> - At short walking distance from nearest community - No lid, and tube perforations present above surface level		
<u>Pumping test</u> - Pump hard to descend in well; well clogged due to combination of clay, sand and water - Discharge rates very low during test - To improve discharge, test multiple times applied with increased position of pump suction - No drawdowns perceived, pumping test aborted		

Figure B.9: Fieldwork fact-sheet: Nungo

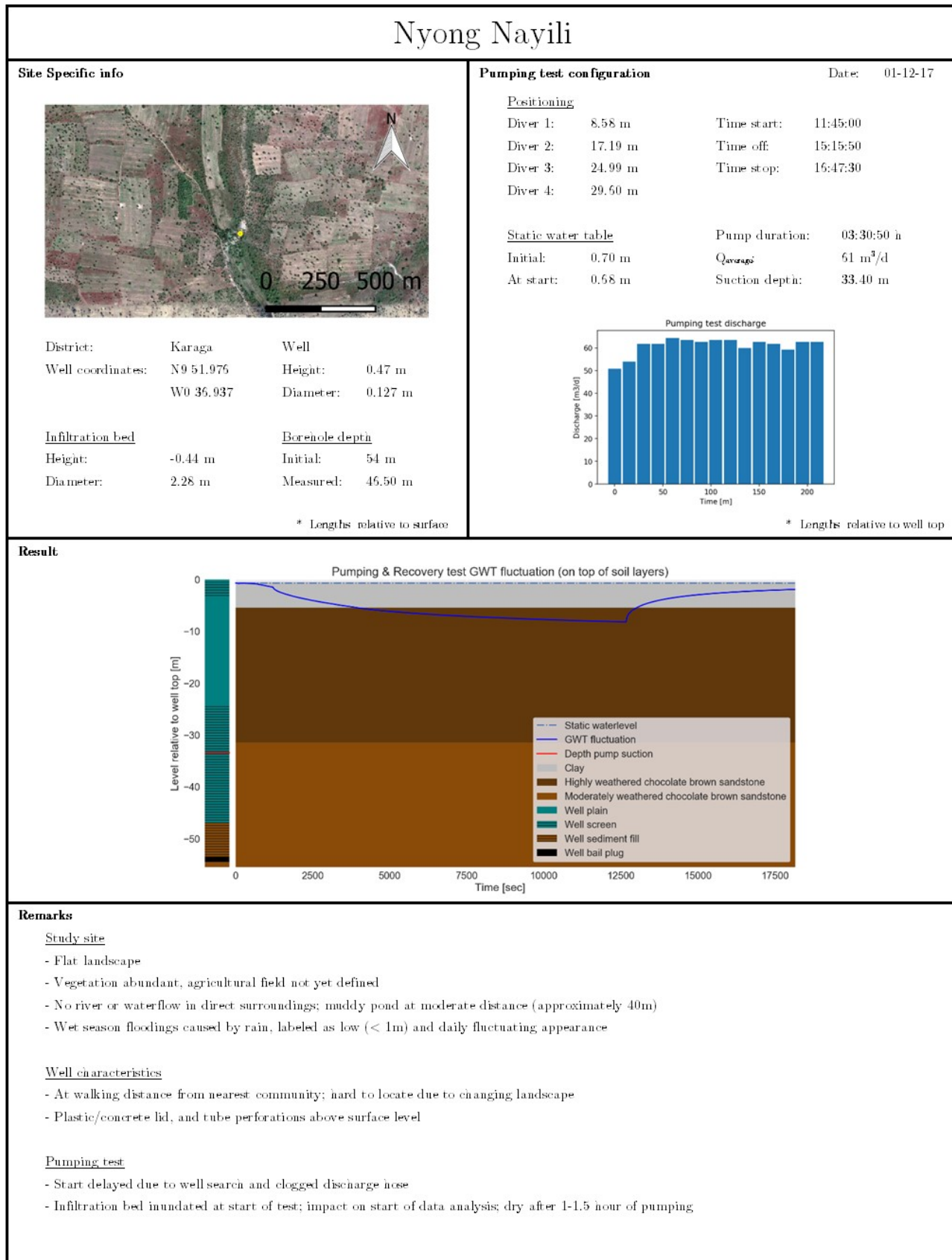


Figure B.10: Fieldwork fact-sheet: Nyong Nayili

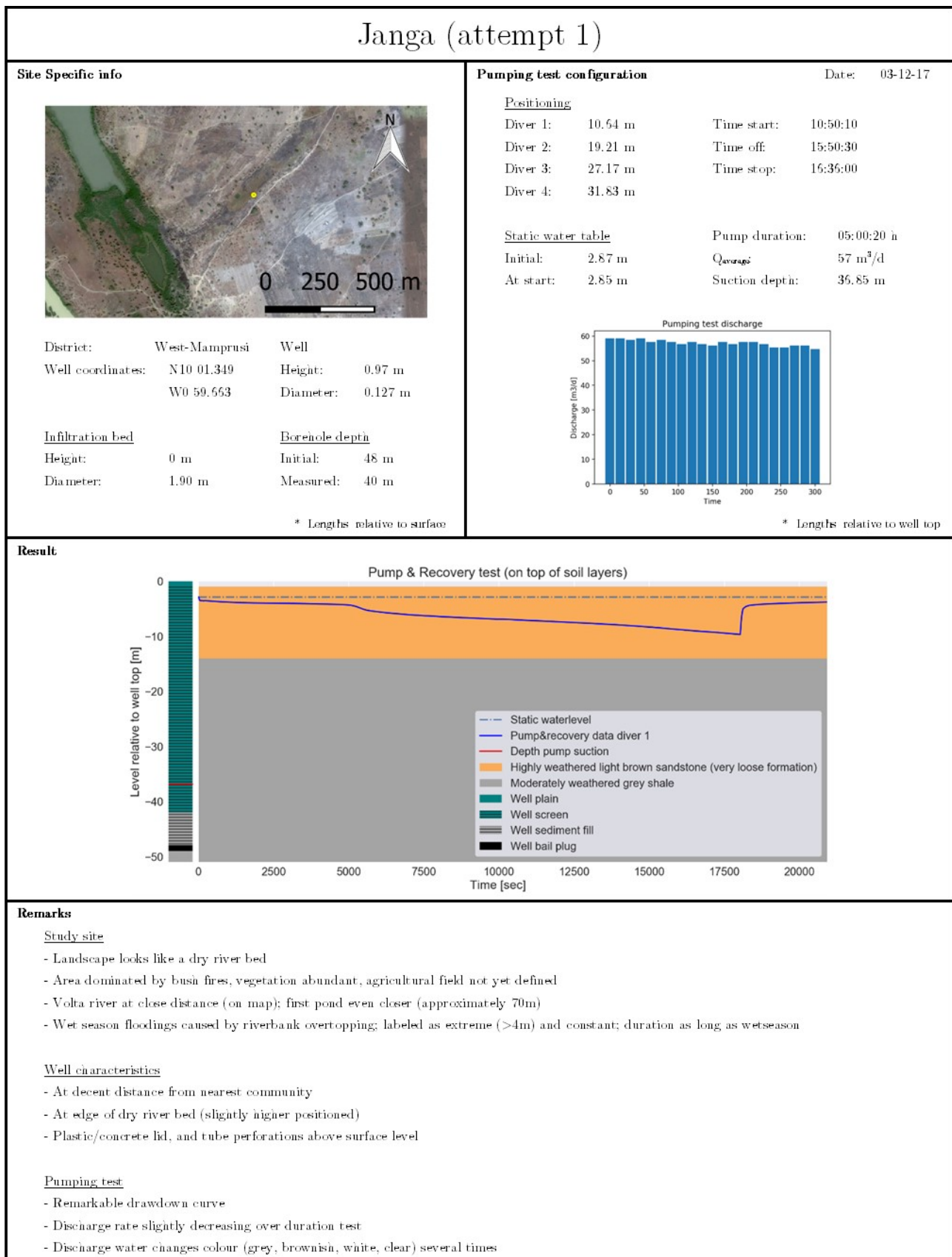


Figure B.11: Fieldwork fact-sheet: Janga (attempt 1)

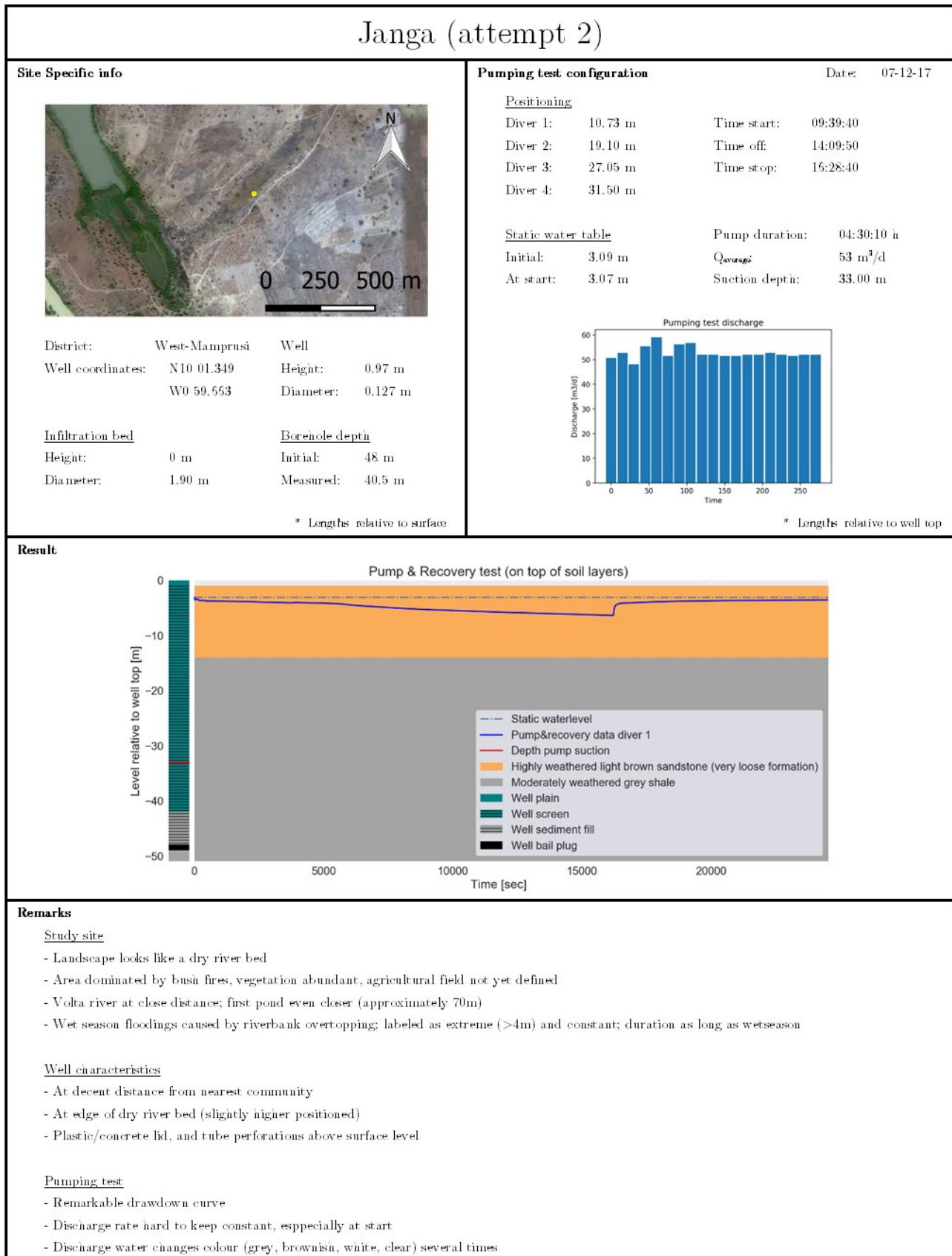


Figure B.12: Fieldwork fact-sheet: Jamga (attempt 2)

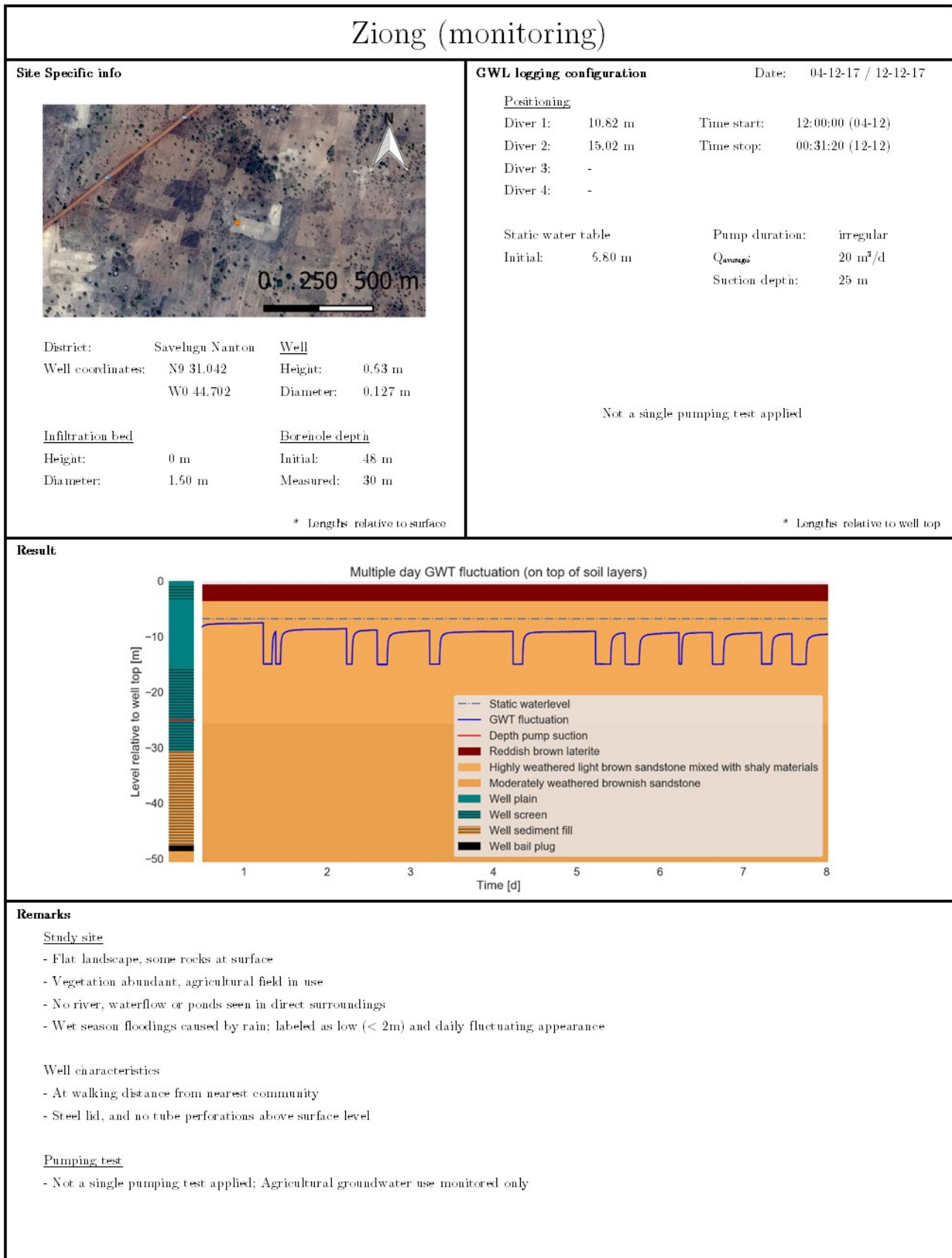


Figure B.13: Fieldwork fact-sheet: Ziong (location of monitoring)

C

588

589

Extense report - Fieldwork data analysis

590 This appendix accommodates a complete overview in fieldwork data analysis. Each location specific dataset
591 is analysed by a distinction in method (analytical Theis's method (single layer), Fmin-RMSE and TTIm Cal-
592 ibrate) and theoretical model (single layer, double layer, partially penetrating double layer). In the TTIm
593 analysis an additional distinction is made between analysis by the use of (a) actual borehole storage and no
594 well resistance, (b) optimal borehole storage and no well resistance, (c) actual borehole storage and opti-
595 mal well resistance, (d) optimal borehole storage and optimal well resistance. Result is the location specific
596 dataset analysis subjected to 25 different approaches; analytical (1x), Fmin-RMS (4x3 = 12x) and TTIm Cal-
597 ibrate (4x3 = 12x). Outcomes in geohydrological parameter values can be found in the tables and figures
598 below.

599 **C.1. Bingo - overview**

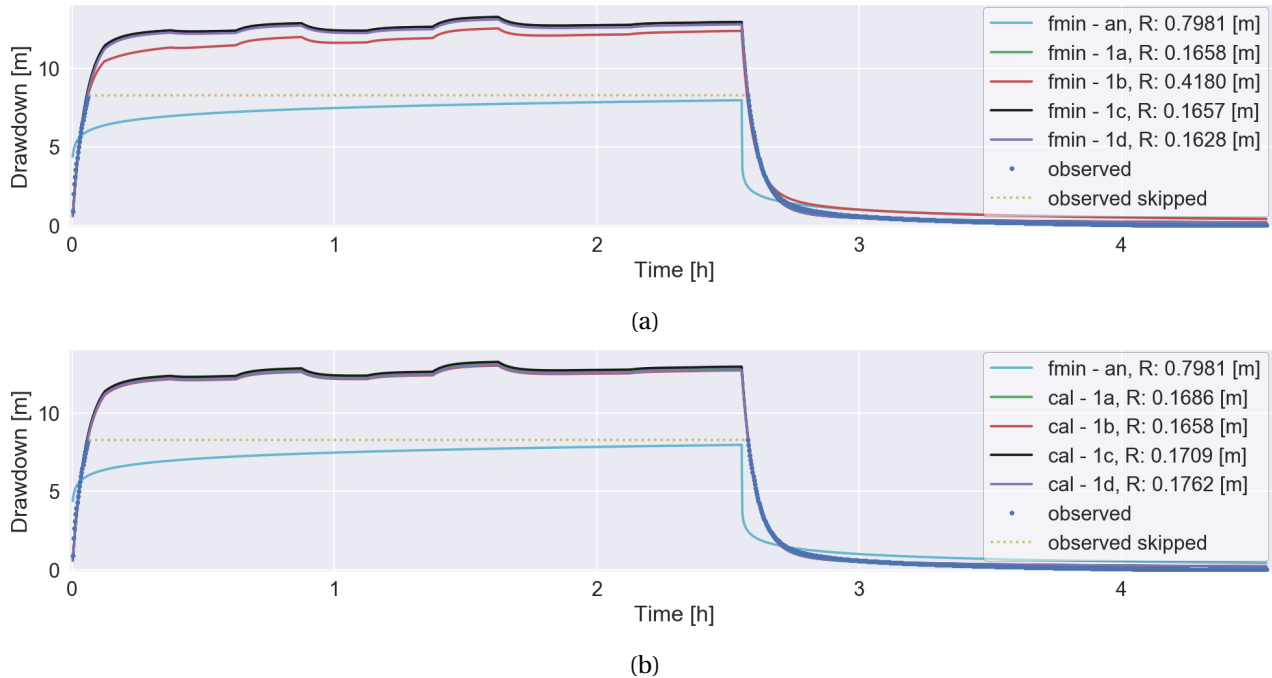


Figure C.1: Bingo single layer fieldwork data analysis by the optimization (a) fmin-RMSE method and (b) TTIm calibration method

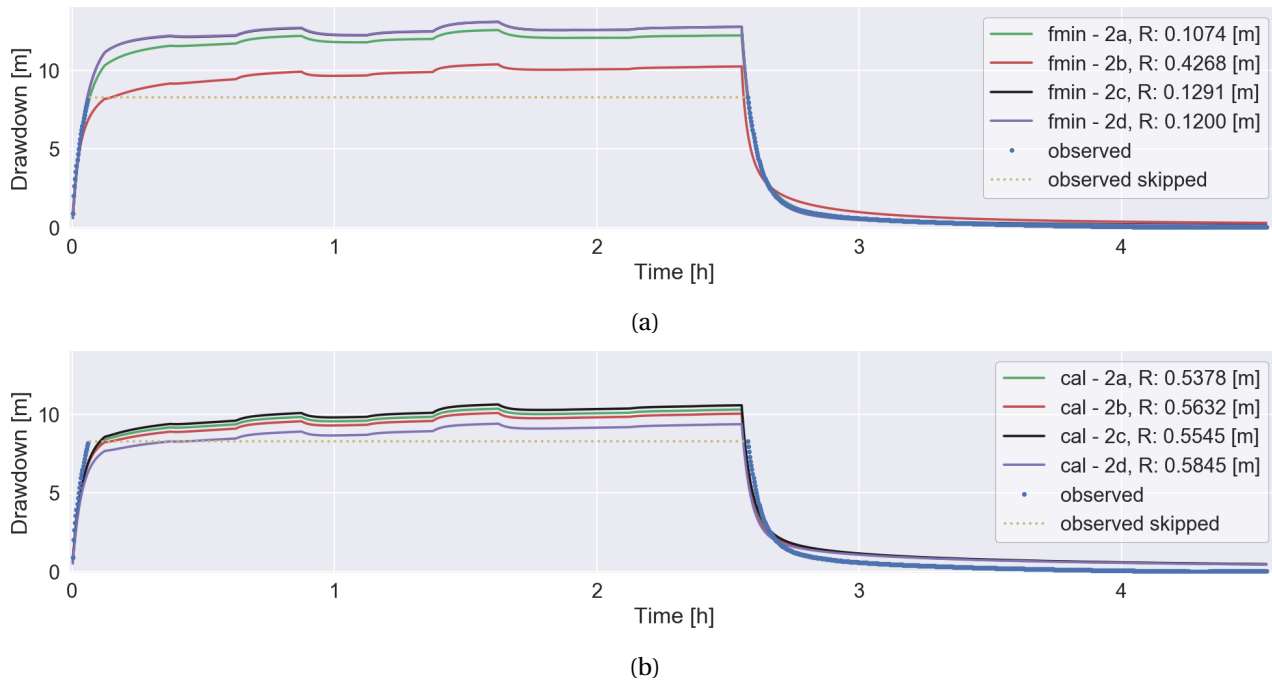


Figure C.2: Bingo double layer fieldwork data analysis by the optimization (a) fmin-RMSE method and (b) TTIm calibration method

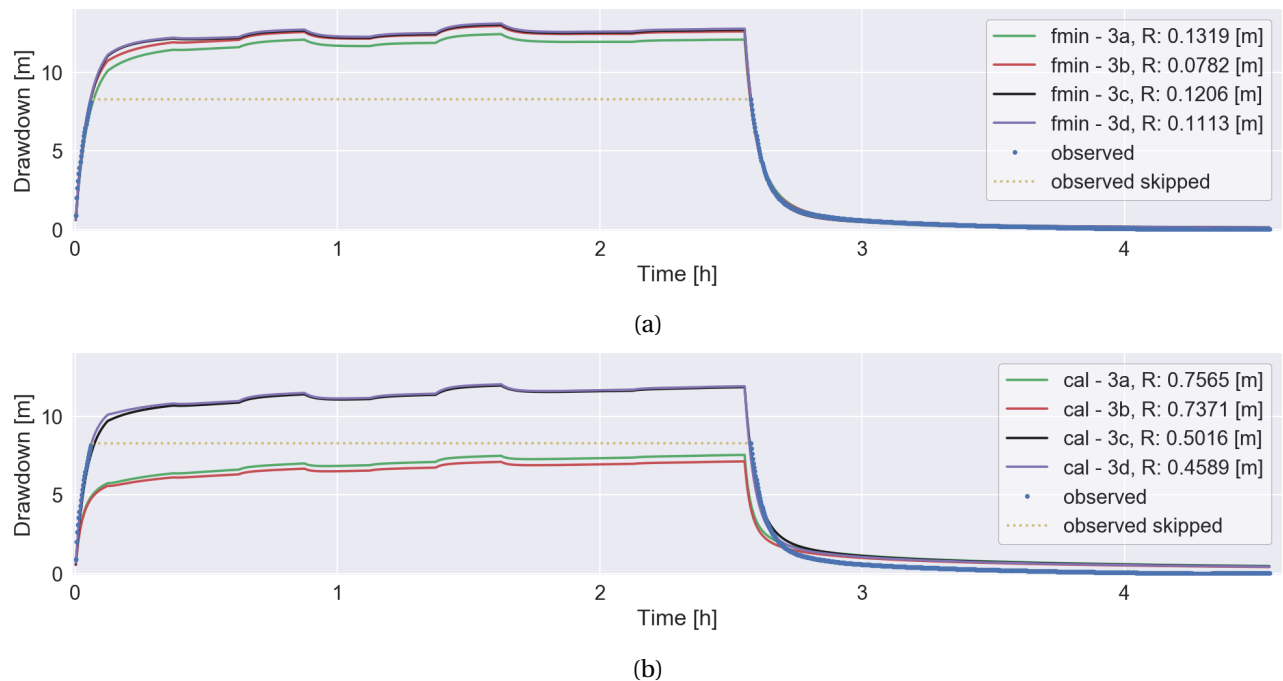


Figure C.3: Bingo partially penetrating double layer fieldwork data analysis by the optimization (a) fmin-RMSE method and (b) TTim calibration method

C.2. Nungo - overview

600
601 Gained fieldwork data at the location Nungo not sufficient for the analysis of geohydrological parameter
602 values.

603 **C.3. Nyong Nayili - overview**

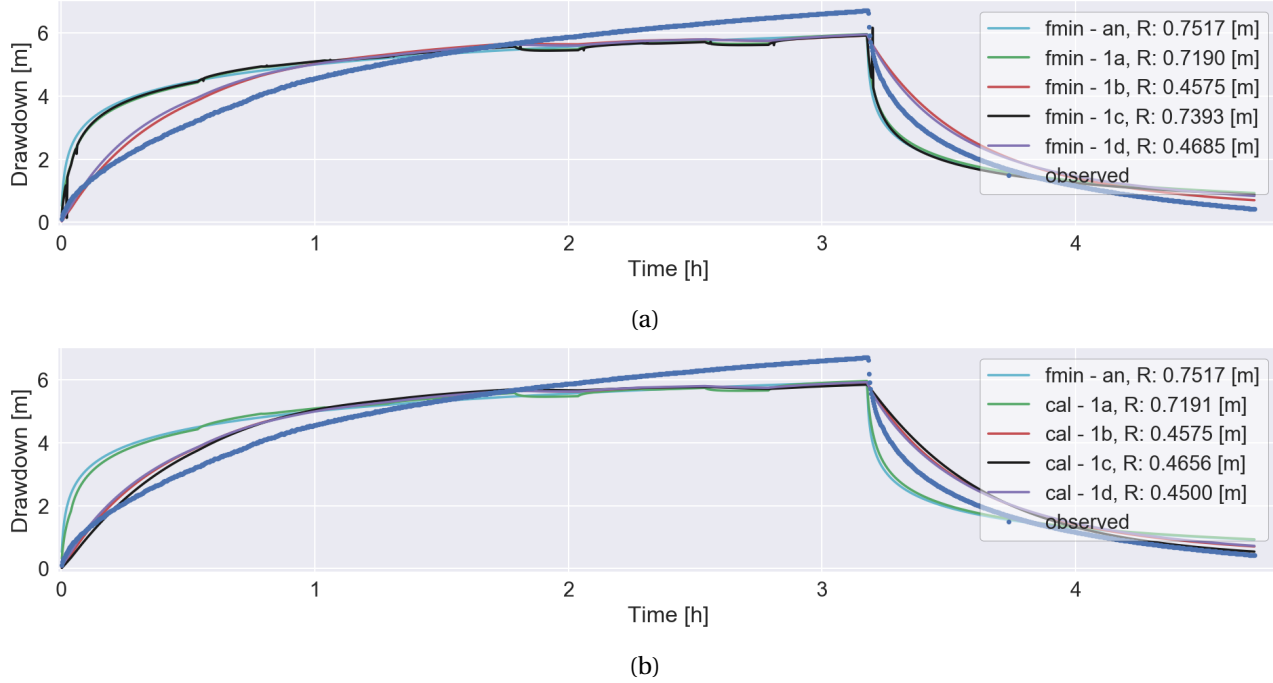


Figure C.4: Nyong Nayili single layer fieldwork data analysis by the optimization (a) fmin-RMSE method and (b) TTIm calibration method

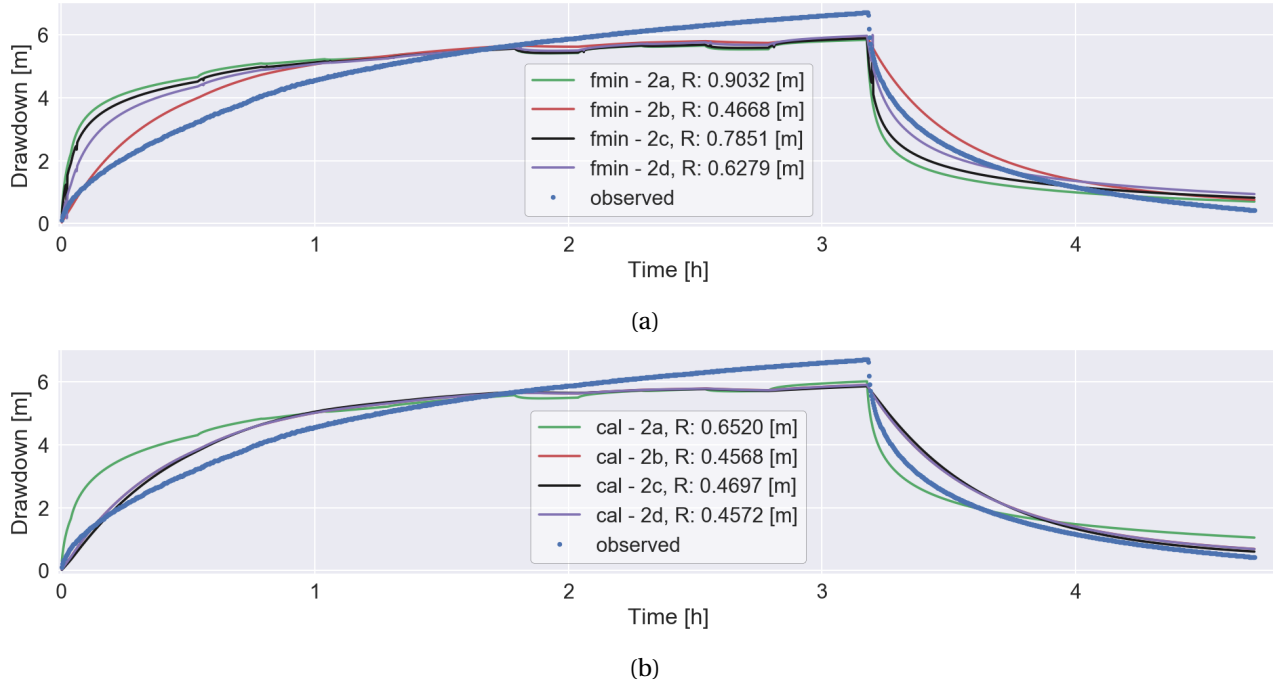


Figure C.5: Nyong Nayili double layer fieldwork data analysis by the optimization (a) fmin-RMSE method and (b) TTIm calibration method

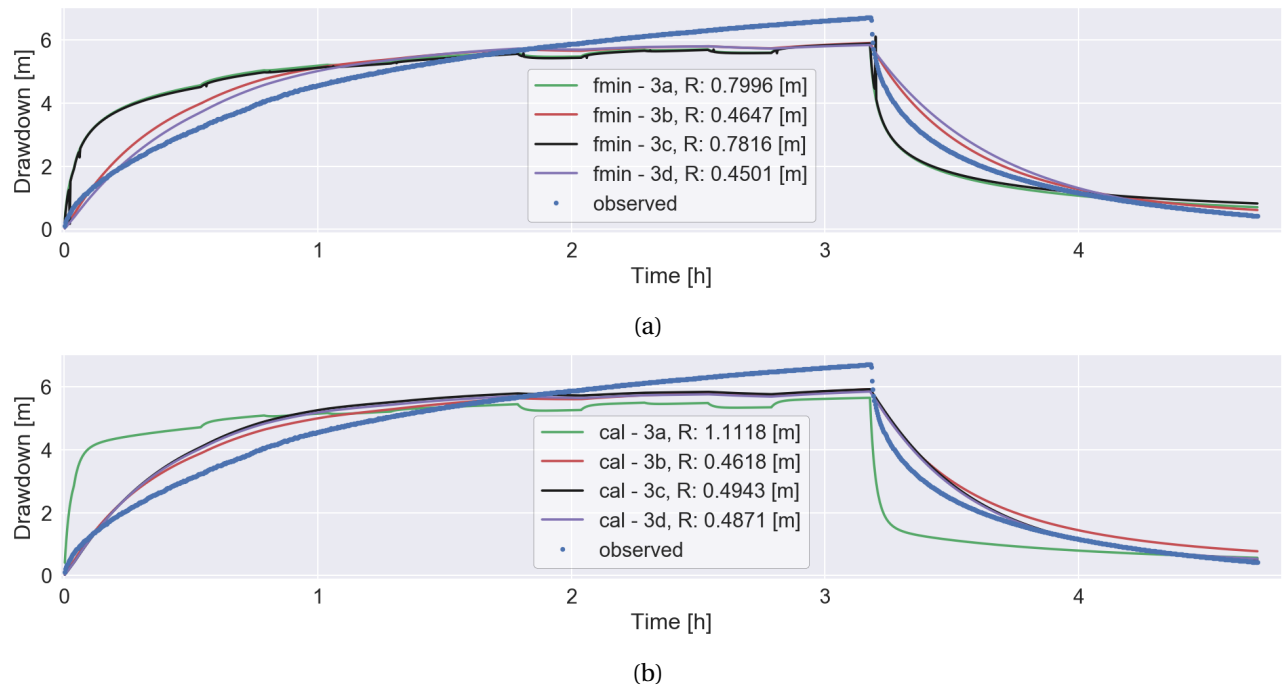
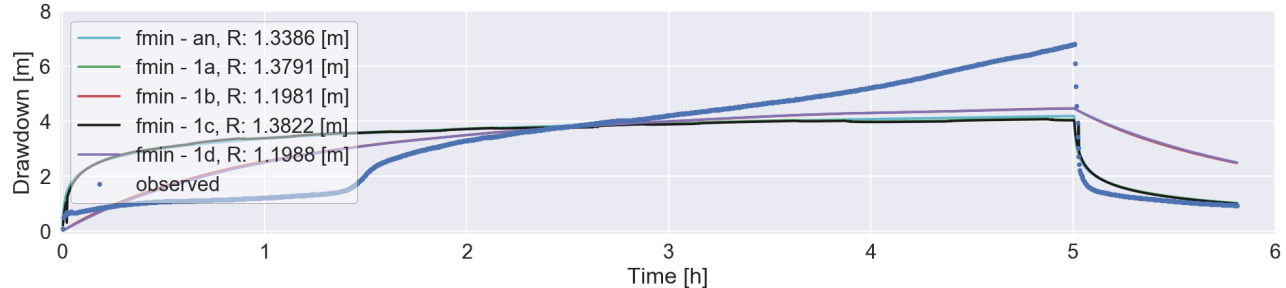
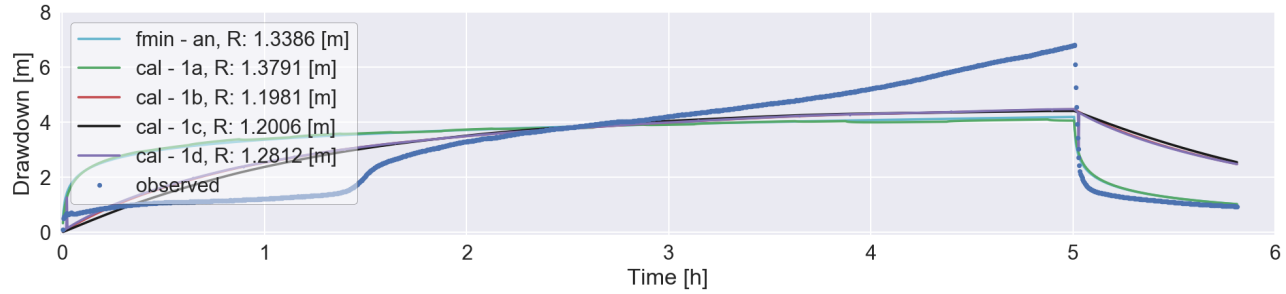


Figure C.6: Nyong Nayili partially penetrating double layer fieldwork data analysis by the optimization (a) fmin-RMSE method and (b) TTIm calibration method

604 C.4. Janga first attempt - overview

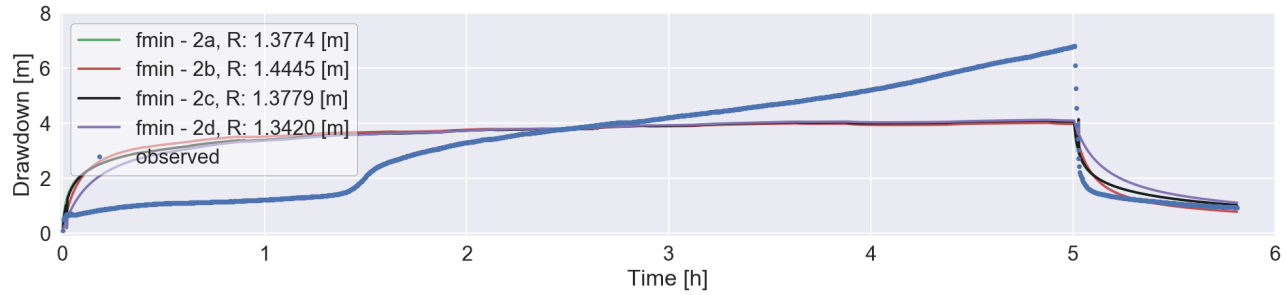


(a)

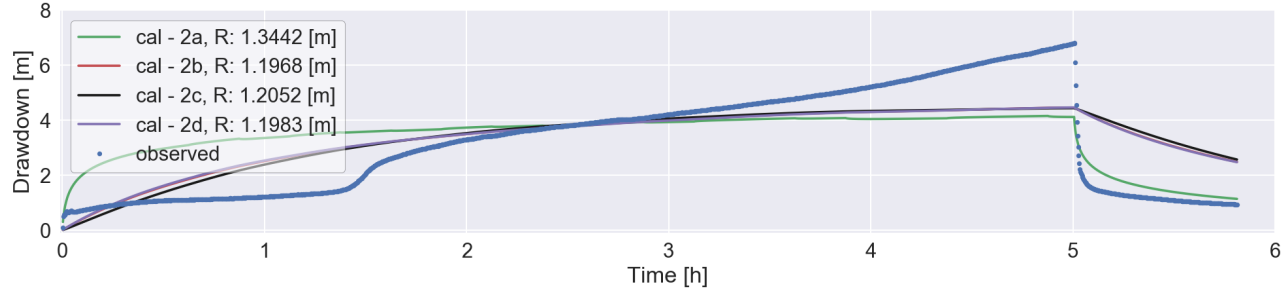


(b)

Figure C.7: Janga first attempt single layer fieldwork data analysis by the optimization (a) fmin-RMSE method and (b) TTim calibration method



(a)



(b)

Figure C.8: Janga first attempt double layer fieldwork data analysis by the optimization (a) fmin-RMSE method and (b) TTim calibration method

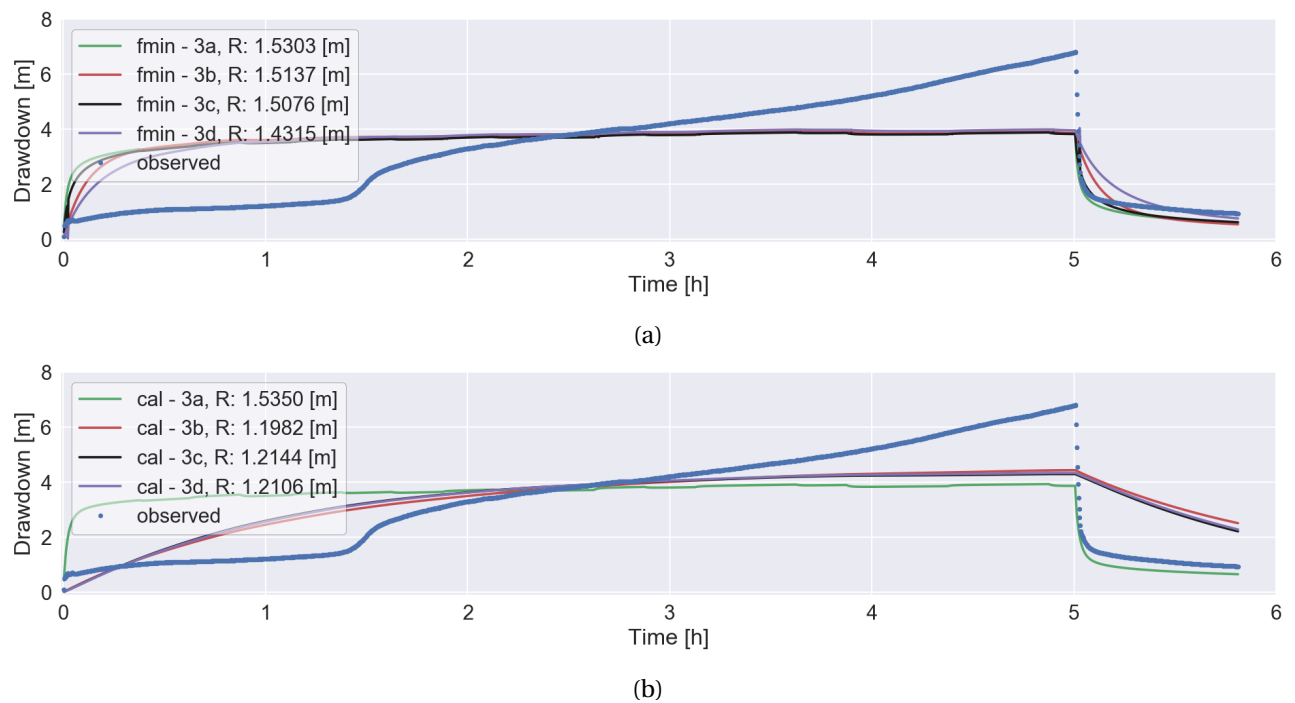
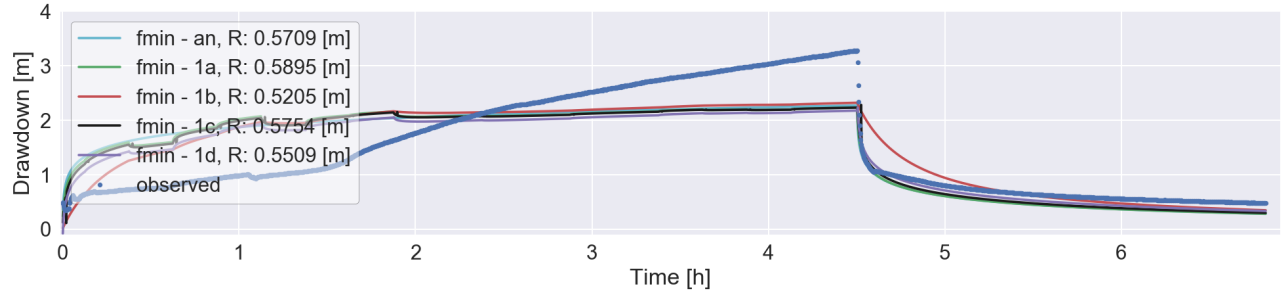
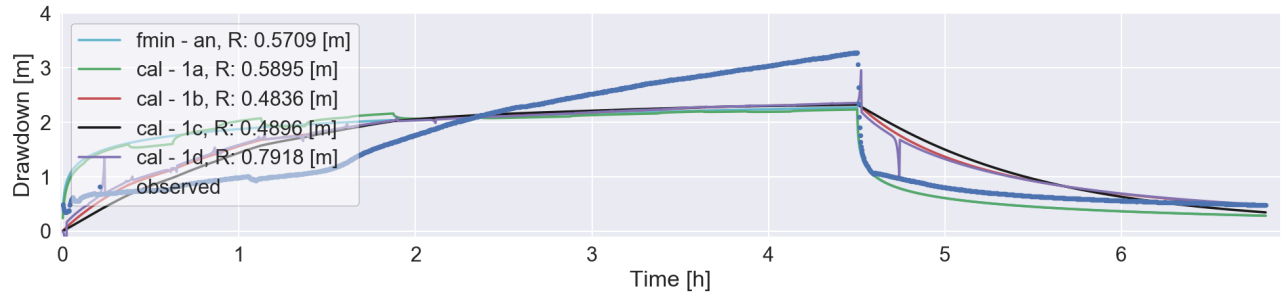


Figure C.9: Janga first attempt partially penetrating double layer fieldwork data analysis (a) fmin-RMSE method and (b) TTIm calibration method

605 **C.5. Janga second attempt - overview**

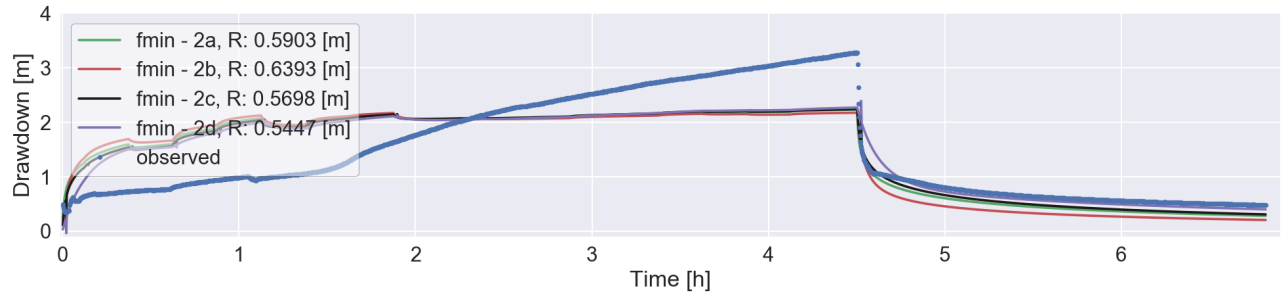


(a)

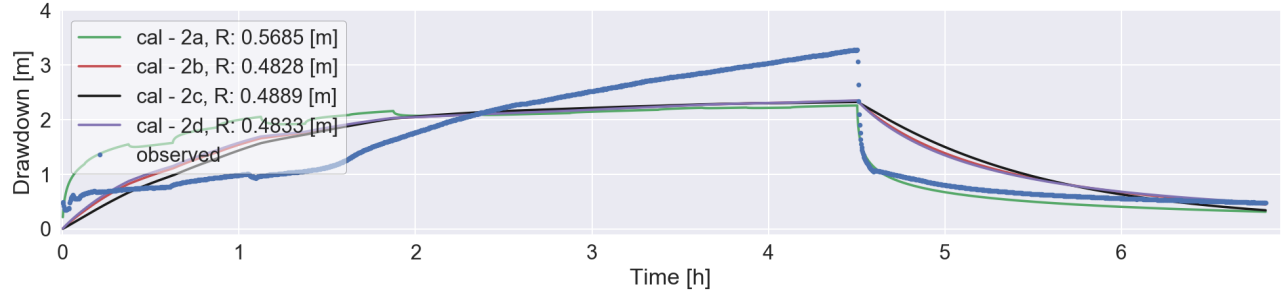


(b)

Figure C.10: Janga second attempt single layer fieldwork data analysis by the optimization (a) fmin-RMSE method and (b) TTIm calibration method



(a)



(b)

Figure C.11: Janga second attempt double layer fieldwork data analysis by the optimization (a) fmin-RMSE method and (b) TTIm calibration method

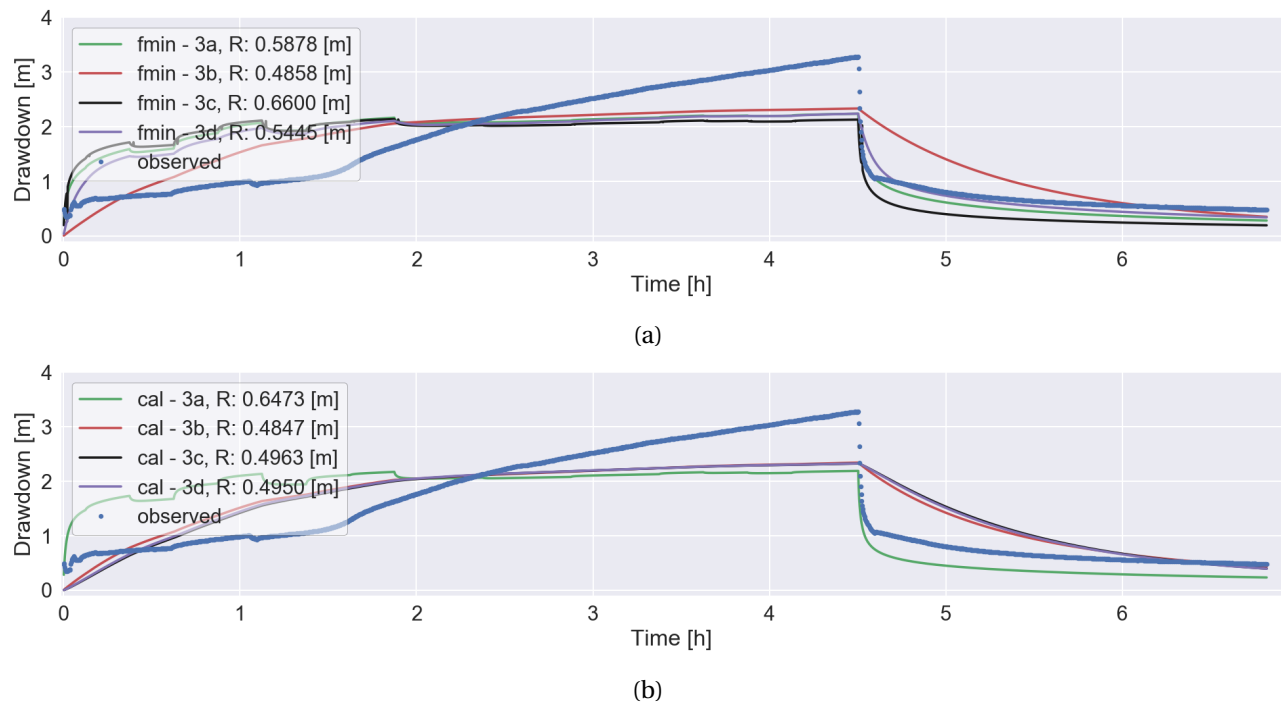
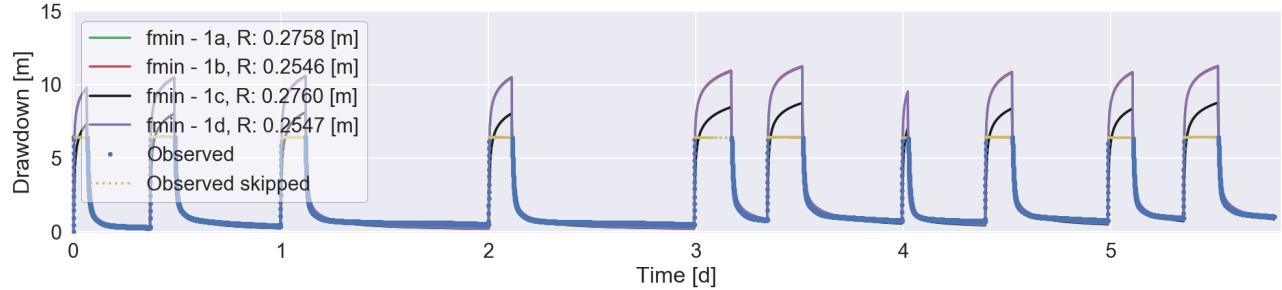
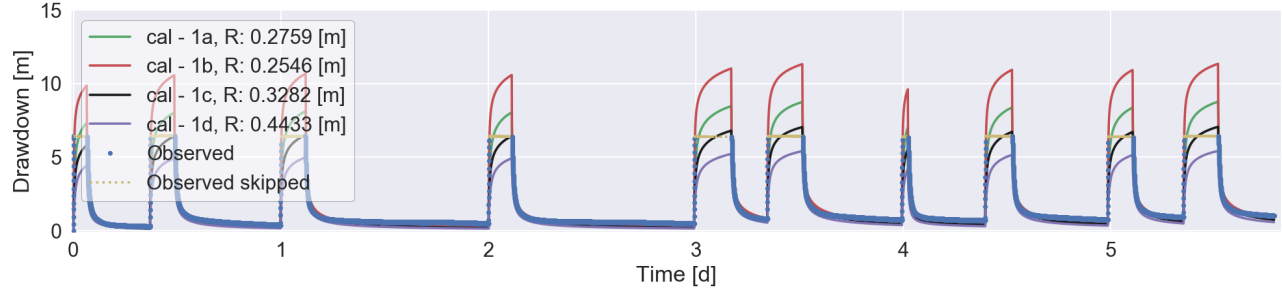


Figure C.12: Janga second attempt partially penetrating double layer fieldwork data analysis by the optimization (a) fmin-RMSE method and (b) TTIm calibration method

606 C.6. Ziong - overview

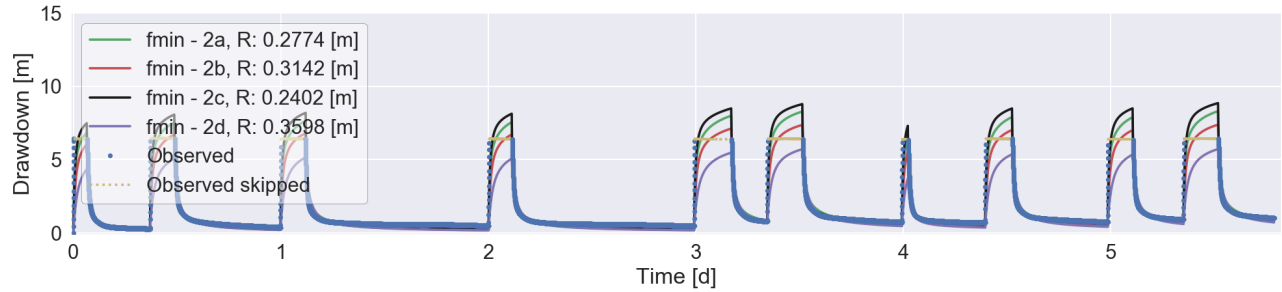


(a)

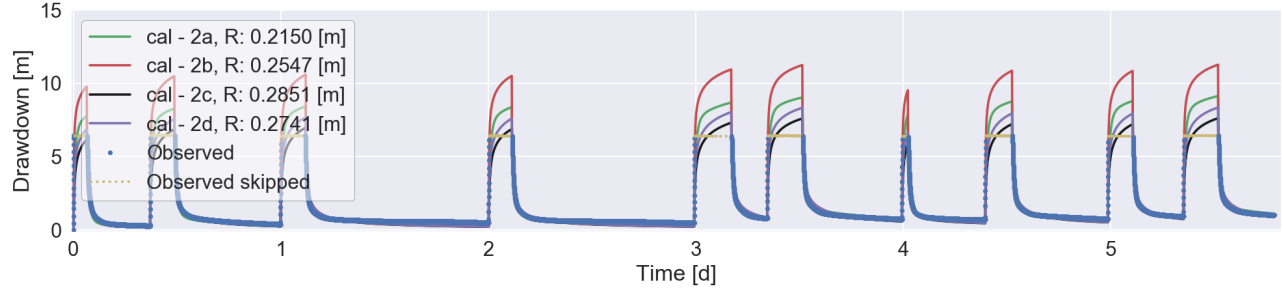


(b)

Figure C.13: Ziong single layer fieldwork data analysis by the optimization (a) fmin-RMSE method and (b) TTIm calibration method



(a)



(b)

Figure C.14: Ziong double layer fieldwork data analysis by the optimization (a) fmin-RMSE method and (b) TTIm calibration method

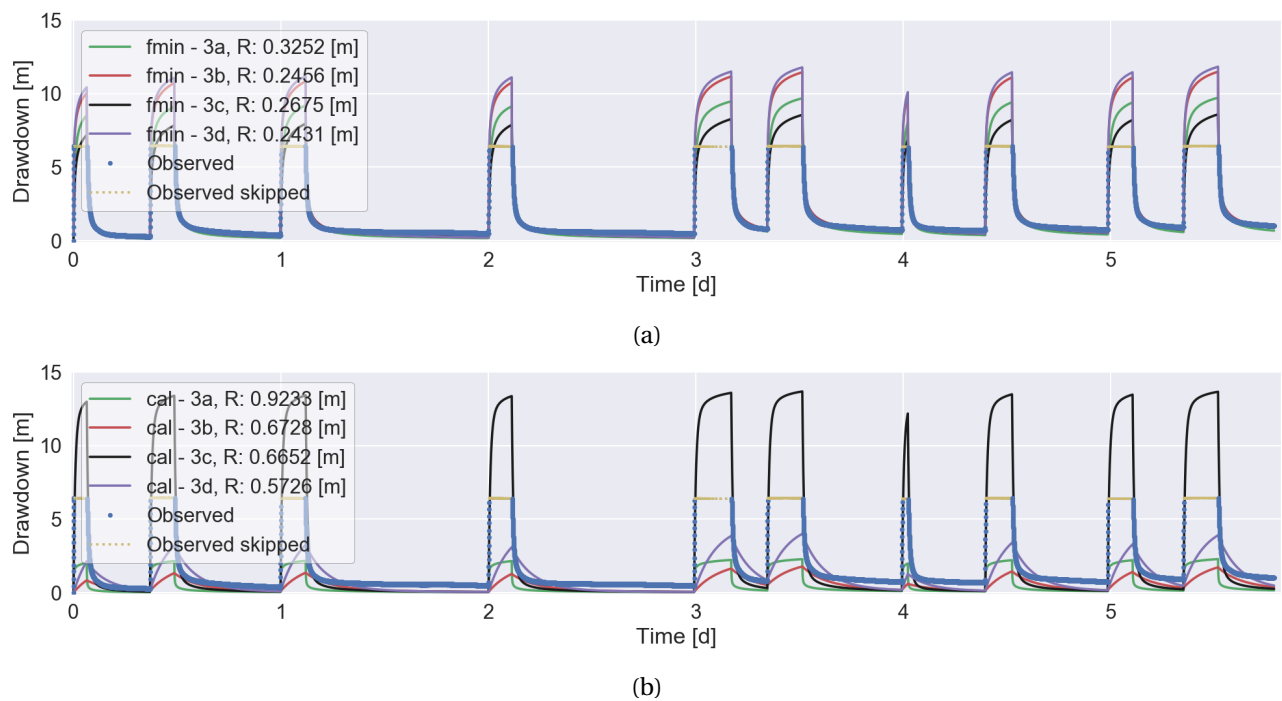


Figure C.15: Ziong partially penetrating double layer fieldwork data analysis by the optimization (a) fmin-RMSE method and (b) TTim calibration method

D

607

608

Modflow radial conversion

609 Introduction

610 The general thesis topic is pointed at the groundwater flow around a well. Due to seasonal circumstances
611 the same well acts both as extraction and injection well. Direction of groundwater flow is alternately pointed
612 towards and away from the well. This phenomenon can be simulated straightforward by the use of the
613 USGS's modular hydrologic model MODFLOW. To generate adequate results in groundwater fluctuations
614 high model accuracies are desirable, especially close to the well. The model preferably accommodates a
615 fine-meshed grid by the implementation of a multitude of rows and columns. As a consequence model
616 runtimes will last long.

617 However, groundwater flow around a well can (under specific conditions) be approached as a phenomenon
618 of radial symmetry. Minor radial parameter conversions can reduce the number of dimensions in the MOD-
619 FLOW model. A modification that reduces model runtimes substantially (Langevin, 2008). The section be-
620 low contains a detailed description of the required radial scaling of parameters, as applied in this thesis. In
621 addition, three examples are included to test and compare the radial scaled model performance.

622 Theoretical method

623 MODFLOW is naturally based on rectangular geometry. Without the inclusion of specific adjustments this
624 results in (multi layered) rectangular models. Model shapes not by definition necessary in the case of a
625 well simulation. Under the assumption of subsurface conditions to be homogeneous and the absence of
626 elements disturbing the regional hydraulic gradient it is possible to interpret the groundwater flow around
627 a well as a phenomenon strictly cylindrical. Assumptions on which one would approach well flow model
simulation as being axially symmetric (Figure D.1).

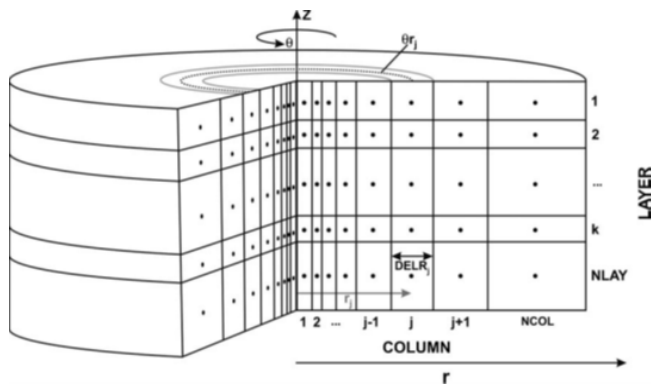


Figure D.1: Schematic of an axially symmetric model (Langevin, 2008)

628

629 The in figure D.1 displayed cylindrical approach of a well model can be simulated by an MODFLOW model
630 (rectangular geometry) which accommodates one or more layer(s), one row only and multiple columns. In
631 this single row model it is assumed the well is included in the first column. Moreover, the single row should

act as the representation of a subsurface slice. This is achieved by the radial modification of multiple parameters. Radial parameter scaling guarantees the conversion of a rectangular (single row) MODFLOW model into a fictive radial model. Elaborating on the explanation of Langevin (2008) the following parameters become radial dependent:

$$K_h \rightarrow K_{h,j}^* = K_{h,j} \theta r_j \quad (\text{D.1})$$

$$K_v \rightarrow K_{v,j}^* = K_{v,j} \theta r_j \quad (\text{D.2})$$

$$S_s \rightarrow Ss_j^* = Ss_j \theta r_j \quad (\text{D.3})$$

$$S_y \rightarrow Sy_j^* = Sy_j \theta r_j \quad (\text{D.4})$$

$$n \rightarrow n_j^* = n_j \theta r_j \quad (\text{D.5})$$

Where K_h and K_v represent the horizontal and vertical hydraulic conductivity, S_s is the specific storage, S_y is the specific yield (phreatic storage) and n is the porosity. Scaled parameters modification is highlighted by the introduction of the superscript *. As visible by the subscript j the parameters hereby become column (radial) dependent. r_j is the radial distance between column j and the well (column 1) and θ is the angle of the representing slice. For the purpose of radial scaling θ covers a complete ring; $\theta == 2\pi$.

Main advantage of the implementation of the radial parameter conversion is the reduction in model dimensions. At local scale (close to well) the model can contain a detailed meshed-grid without the emergence of excessive model runtimes. Moreover the parameter is applied within the common modelling program MODFLOW itself, no specialized programs are required. However, it has to be mentioned the circular model approach can only be applied under the specific assumptions of radial symmetry (Langevin, 2008).

Test application

To validate the radial scaled model performance, a total of three fictive test exercises are applied. In these exercises a comparison is made between the radial scaled model (Figure D.2c) and two natural rectangular based MODFLOW models (Figure D.2a and Figure D.2b). The rectangular MODFLOW model is the most straightforward. Due to the squared shape deviations in model outcome are expected. Whereas the rectangular round MODFLOW model is manually circularized. This model accommodates the gradual increase in flow area in the radial direction. Based on Langevin (2008) it is expected the rectangular round model should approximate radial model outcomes.

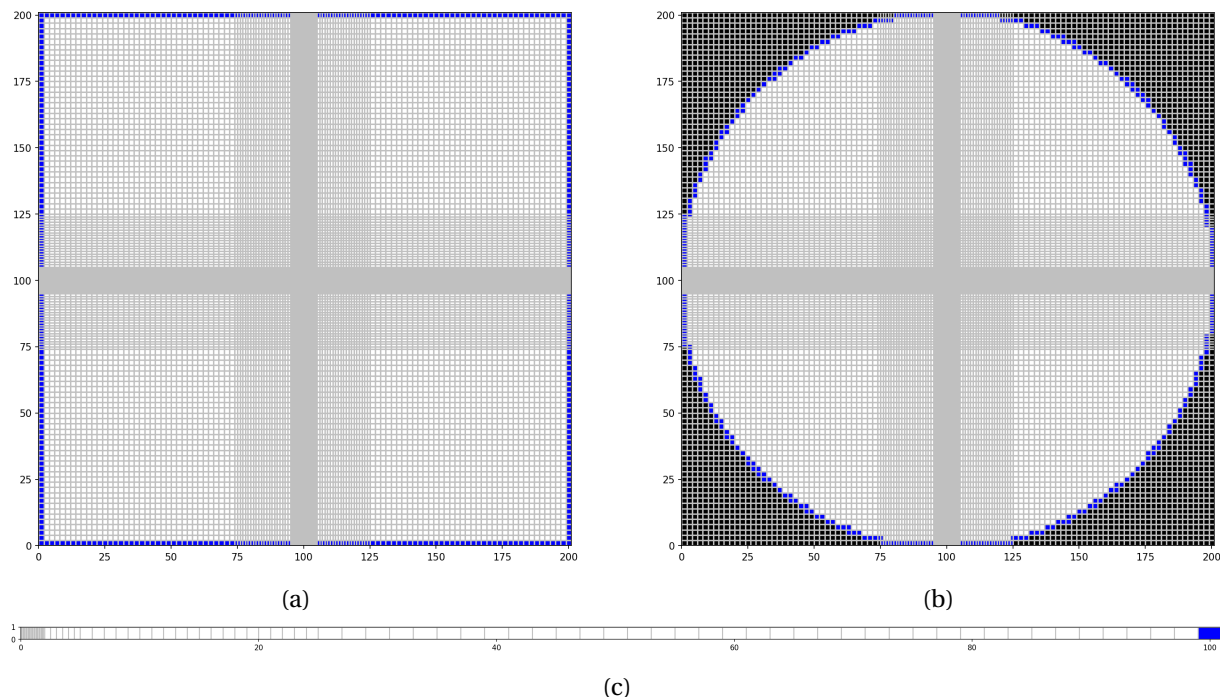


Figure D.2: MODFLOW topview schematisation of a: (a) Rectangular model, (b) Rectangular round model and (c) Single row model
 (grey = cell boundary, red = well position, blue = boundary condition, black = inactive cell)

655 The exercises applied deliberately show strong similarities with the first two test problem cases described
 656 by Langevin (2008). In terms of content the exercises are designed with the same set of parameters, making
 657 it possible to validate the results in general. As an exception a small deviation is applied in terms of grid def-
 658 inition. In these exercises the cell sizes increase (grouped) stepwise based on an increasing (radial) distance
 659 from the well. By the use of the cell sizes 0.1 (20x), 0.5 (6x), 1.0 (20x) and 2.0 m (38x) a total model length
 660 (radial length) of 101 m is simulated. This grid structure is applicable on the single row (radial) model. The
 661 rectangular and rectangular round model accommodate a same and corresponding grid structure, as visible
 662 in the model top views of figure D.2.

D.1. Test 1: Steady flow to a fully penetrating well in confined aquifer

The steady state solution of a confined aquifer fully penetrated by a well is applied as a first MODFLOW model performance test. The exercise schematic configuration is depicted in the overview of figure D.3. The case is characterized by its simplicity, making it an exercise ideally suitable for the comparison against the analytical solution. Thiem's method (Equation D.6) is applied as the analytical drawdown solution for radial well flow in a confined aquifer (Krusseman & de Ridder, 2000):

$$S_j = \frac{Q \ln(\frac{r_2}{r_j})}{2\pi K_{(h)} H} \quad (\text{D.6})$$

Where S_j is the drawdown in column j , Q is the discharge, $r_2 = 100$ m (constant head at a distance of in this case 100 m from the well), r_j is the radial distance between column j and the well (column 1), $K_{(h)}$ is the horizontal hydraulic conductivity and H is the aquifer thickness.

Decline in groundwater head due to well behaviour can also be expressed directly by the use of the analytical discharge potential (strack, 1989), as depicted in (Equation D.7). Applied on confined conditions it is assumed $H = h_0$ (Source?? geo1). As a result confined heads can be determined by the application of equation D.9. Outcomes in head are in complete correspondence with the drawdown calculated by Thiem's method.

$$\phi_j = \frac{Q}{2\pi} \ln\left(\frac{r_j}{R}\right) + \phi_0 \quad (\text{D.7})$$

$$\phi_0 = k_h H h_0 \quad (\text{D.8})$$

$$h_j = \frac{\phi_j}{k_h H} \quad (\text{D.9})$$

Where ϕ_j is the discharge potential at column j , Q is the discharge, $R = 100$ m (constant head (h_0) at a distance of in this case 100 m from the well), r_j is the radial distance between column j and the well (column 1), $K_{(h)}$ is the horizontal hydraulic conductivity and H is the aquifer thickness.

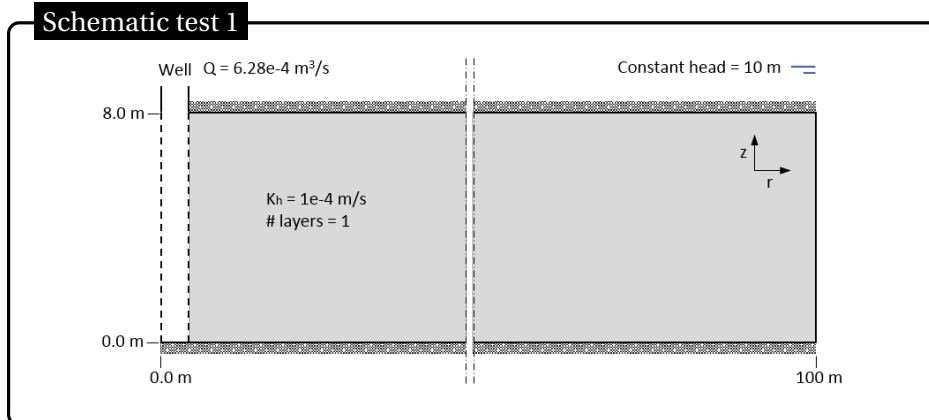


Figure D.3: Schematic test 1

The rectangular MODFLOW model overestimates drawdown (modelled heads are slightly lower) compared to the analytical solution. This difference can be explained by the rectangular shape of the model; imposed boundary condition along the model edge (especially the corners) are positioned 'outside' the defined radial boundary of 100 m from the well. The rectangular round model works around this inconvenience, and already shows more similarities with the analytical solution. Some deviation in the first meter(s) around the well still exist, which can potentially be attributed to the cell structure. These minor deviations are no longer present by the application of the radial scaled (single row) model. Regardless the (radial) position, modelled heads and drawdown are identical to the analytical solution. A first indication the radial scaled MODFLOW model is preferential applicable on this thesis purposes.

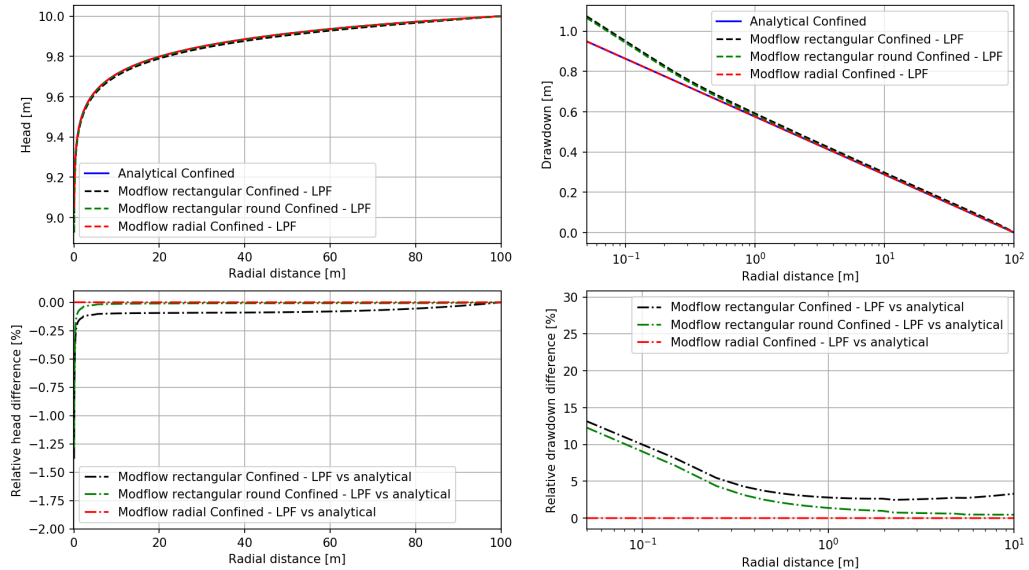


Figure D.4: Results test 1

D.2. Test 2: Steady flow to a fully penetrating well in unconfined aquifer

Example exercise two (Figure D.5) accommodates the same test problem as depicted in test 1, only exception is the transition towards unconfined aquifer conditions. In this example the analytical drawdown solution presented by the Thiem-Dupuit's method for steady-state flow to a fully penetrating well in an unconfined aquifer is used as a reference(Kruseman & de Ridder, 2000):

$$S'_j = \frac{Q \ln(\frac{r_2}{r_j})}{2\pi K_{(h)} D} \quad (\text{D.10})$$

$$S'_j = S_j - \frac{S_j}{2D} \quad (\text{D.11})$$

Where S'_j is the uncorrected drawdown in column j, S_j is the iteratively corrected drawdown in column j, Q is the discharge, $r_2 = 100$ m (constant head at a distance of 100 m from the well), r_j is the radial distance between column j and the well (column 0), $K_{(h)}$ is the horizontal hydraulic conductivity and D is the thickness between aquifer bottom and constant head. For the purposes of this exercise the analytical drawdowns are iteratively determined with a precision of 1e-6.

Also under unconfined conditions the analytical discharge potential (Equation D.12) can be applied (Strack, 1989). Only exception, compared to the confined conditions, is the minor change in head derivation, visualised in D.14. Major advantage, with respect to the analytical Thiem-Dupuit's method, is the absence of the iterative head derivation process. Result is the analytical calculation of even more accurate heads by the application of the discharge potential.

$$\phi_j = \frac{Q}{2\pi} \ln\left(\frac{r_j}{R}\right) + \phi_0 \quad (\text{D.12})$$

$$\phi_0 = \frac{1}{2} k_h h_0^2 \quad (\text{D.13})$$

$$h_j = \sqrt{\frac{2\phi_j}{k_h}} \quad (\text{D.14})$$

Where ϕ_j is the discharge potential at column j, Q is the discharge, $R = 100$ m (constant head (h_0) at a distance of in this case 100 m from the well), r_j is the radial distance between column j and the well (column 1), $K_{(h)}$ is the horizontal hydraulic conductivity and H is the aquifer thickness.

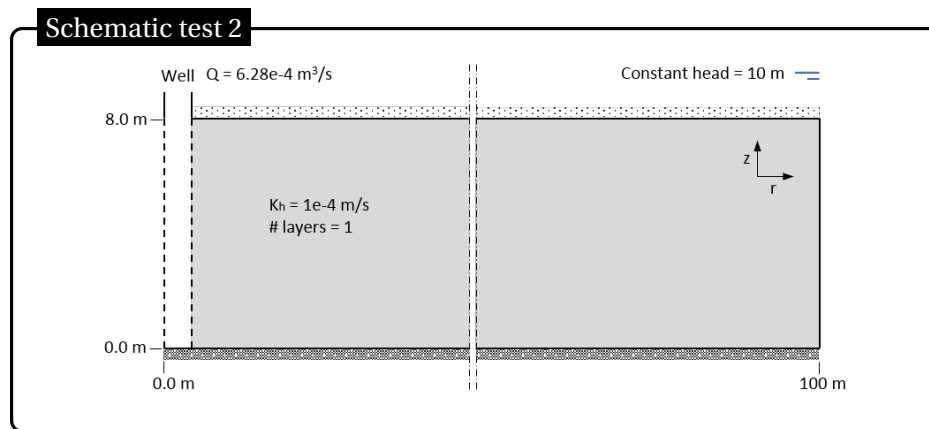


Figure D.5: Schematic test 2

Due to a 10 m constant head boundary the aquifer area of flow is fictive enlarged in the unconfined case (compared to the 8 m aquifer height under confined conditions). In accordance with the solutions in Langevin (2008) overall drawdowns in the unconfined conditions are slightly lower with respect to the confined situation. Model performances of the unconfined example exercise show similar behaviour as the

715 confined example exercise. Differences in modelled and analytical determined heads and drawdowns are
 716 minuscule in general. As expected largest deviations from the analytical solution are present in the MOD-
 717 FLOW rectangular model. The differences in outcome of this model do persist over almost the entire radial
 718 distance from the well, regardless the use of the BCF or LPF package. Although it is only slightly, the use
 719 of the LPF package shows slightly better performance. For the purposes of this thesis the LPF package is
 720 assumed to be preferential in setting the aquifer properties. Application of this package in the MODFLOW
 721 round rectangular model results in improved model results, however deviations do continue to exist. In
 722 contrast with the confined exercise (D.1) application of the radial scaled MODFLOW model under uncon-
 723 fined aquifer conditions deviations from the analytical solution are still present. Modelled drawdowns show
 724 strong similarities with the uncorrected analytical solution. Moreover, relative to the analytical solution the
 725 absolute radial scaled MODFLOW model outcomes performs most accurately. Making the radial scaled
 726 (single row) MODFLOW model suitable for the unconfined aquifer conditions of this thesis.

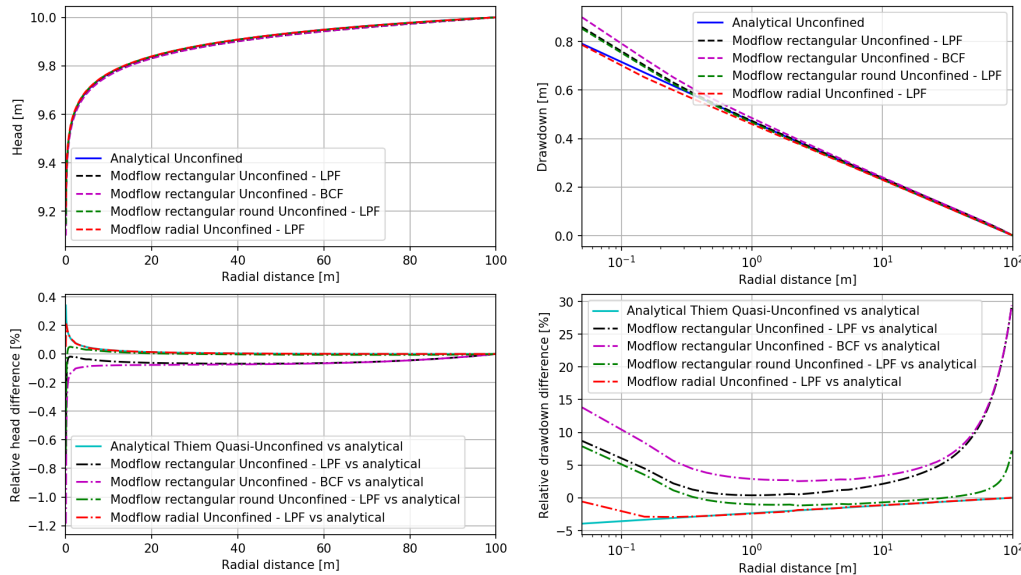


Figure D.6: Results test 2

727 D.3. Test 3: Unsteady flow to a partially penetrating well in unconfined aquifer

728 As a final exercise the different MODFLOW models are subjected to a more complicated case (Figure D.7).
 729 This specific exercise includes all model parameters dependent on radial scaling to test the overall radial
 730 model performance. This case accommodates a well which is partially penetrating the aquifer, making it a
 731 multi-layered problem. Sum up of the fractional discharges of the penetrating layers (48-72) results in the
 732 total well discharge. Moreover the exercise is time dependent. In this case all results are obtained after one
 733 day of groundwater withdrawal.

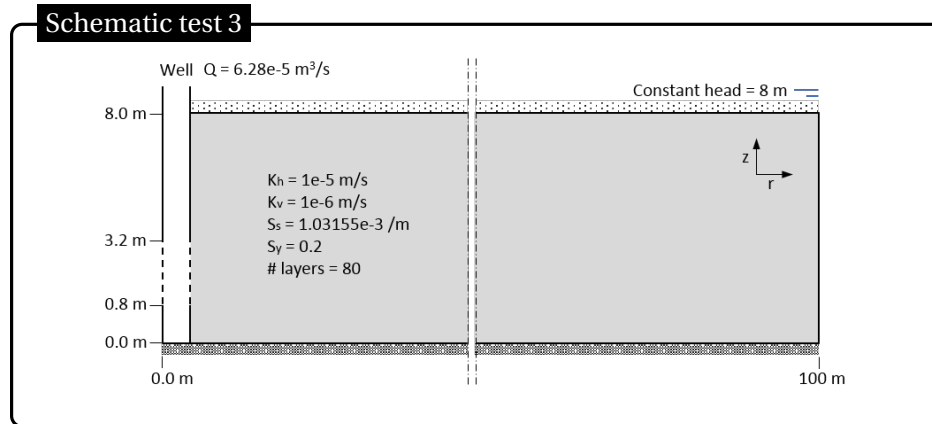


Figure D.7: Schematic test 3

734 Performance of the radial scaled (single row) MODFLOW model is visualized by the head contour plot in fig-
 735 ure D.8. From the perspective of proper comparison results of the different models are in this case shown
 736 at an height of 2.0 m (relative to aquifer bottom) along the entire aquifer (Figure D.9). Outcome of the com-
 737 parative study is a scaled (single row) radial model which performs as expected. With the exception of the
 738 first meter(s) around the well differences between the rectangular round and the radial MODFLOW models
 739 are negligible small. Deviations at close range to the well can be attributed to the chosen grid structure.
 740 Based on the test exercises 1 and 2 it can be assumed the results of the radial model simulates the natural
 741 well behaviour properly. Application of the radial scaled (single row) MODFLOW model with the use of the
 742 LPF package is a relative fast and suitable model for this thesis purposes.

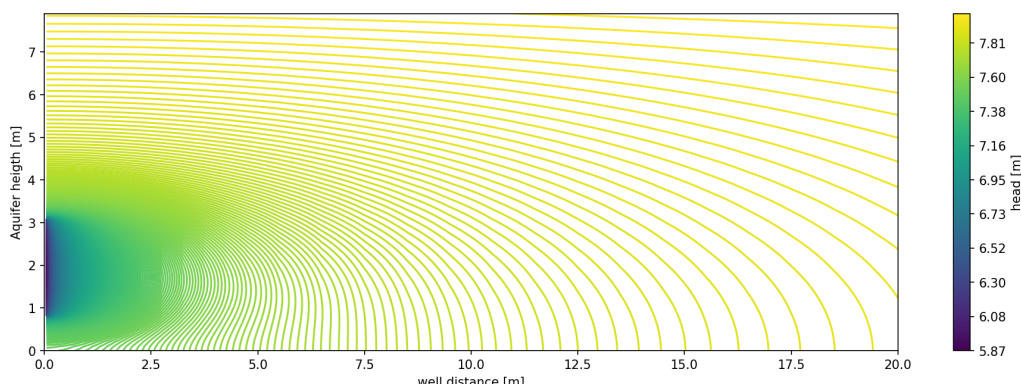


Figure D.8: Results test 3: Cross-section head contour after 1 day of pumping

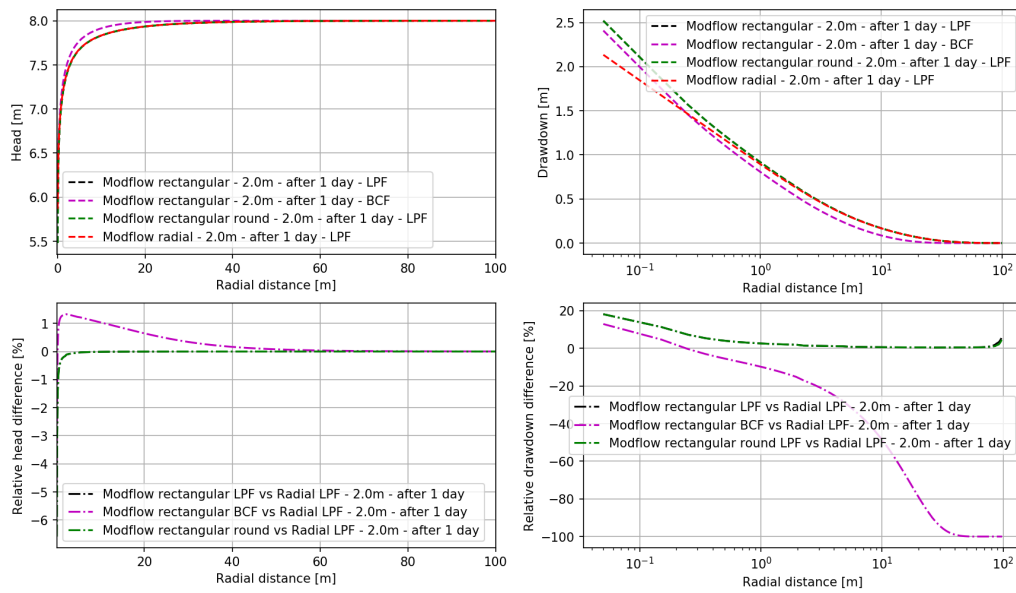


Figure D.9: Results test 3: Head after 1 day of pumping at 2.0m (relative to aquifer bottom)